# Nonlocal analysis of Rayleigh wave with double porosity and dual-phase-lag model

Ismail Haque; Chandra Sekhar Mahato and Siddhartha Biswas\* Department of Mathematics, University of North Bengal, Darjeeling, India

#### Abstract

The purpose of this article is to develop the propagation of Rayleigh waves in a nonlocal thermoelastic isotropic material with double porosity whose surface is subjected to stress free, thermally insulated/isothermal boundary conditions. Linear theory of nonlocal thermoelastic material with double porosity structure is developed within the context of Eringen's theory of nonlocal thermoelasticity. Dual-phase-lag (DPL) model and Lord-Shulman (LS) model of hyperbolic thermoelasticity is developed in the context of nonlocal and double porosity. Energy density function is constructed from the basic variables, and then, constitutive relations are derived, which are used to develop the field equations for an isotropic homogeneous nonlocal thermoelastic material with double porosity. The vector matrix differential equation is obtained by applying the normal mode analysis to the considered equations. Some special cases are also derived from this study which are also compared with the existing results of the various researchers. The effects of voids and nonlocality on different characteristics of Rayleigh waves are presented graphically. This theory seems to be an adequate tool to describe the behaviour of granular materials like rock, soils and manufactured porous bodies. Numerical results for the different characteristics of Rayleigh waves like propagation speed, attenuation coefficient, specific loss and penetration depth are computed numerically. The computer simulated results for copper materials in respect of determinant of Rayleigh wave secular equation, Rayleigh wave velocity, attenuation coefficient, specific loss and propagation speed have been presented graphically.

**Keywords**: Rayleigh waves, nonlocal elasticity theory, dual-phase-Lag (DPL) and Lord-Shulman (LS) models, double porosity.

### 1 Introduction

The nonlocal thermoelasticity theory has attracted the largest attention of many authors because this theory has played an important role in solving many past complications in fracture mechanics. Eringen (1977) developed the problem of a straight-edge dislocation in nonlocal

<sup>\*</sup>Corresponding author: Siddhartha Biswas, Email: siddharthabsws957@gmail.com

elasticity. Eringen (1974) employed the theory of nonlocal thermoelasticity. Eringen (1998) founded a mixture theory of electromagnetism and superconductivity. Eringen (1972) derived a theory of nonlocal elasticity in which constitutive equations are obtained for the nonlinear theory, first through the use of a localised Clausius-Duhem inequality and second through a variational statement of Gibbsian global thermodynamics. Within the framework of Eringen's theory of nonlocal elasticity, Kumar et al. (2021) looked into the linear theory of nonlocal elastic material with double porosity structure. Using the fundamental variables, the energy density function is built. Constitutive relations are then obtained and applied to generate the field equations for an isotropic homogeneous nonlocal elastic material with double porosity. Zhou et al. (2006) investigated the dynamic behavior of a finite crack in functionally graded materials subjected to harmonic stress waves by means of nonlocal theory.

The concept of porous media is a flexible and essential cornerstone in the fields of applied science and engineering. It has numerous uses in the geosciences (hydrogeology, petroleum geology, geophysics), engineering (petroleum engineering, construction engineering), biology and biophysics, material science, filtration, and mechanics (acoustics, geomechanics, soil mechanics, and rock mechanics). Using Nunziato and Cowin's elastic materials with void theory (1979, 1983), Iesan and Quintanilla (2014) developed a theory of thermoelastic solids with a double porosity structure. Puri and Cowin (1985) have derived the plane wave propagation in elastic material with voids and found that three types of plane waves may be propagating at different speeds.

Khalili and Selvaduri (2003) proposed a fully coupled constitutive model for thermo-hydro-mechanical analysis in elastic media with double porosity. Ostoja-Starzewski (2009) discussed the extension of continuum mechanics and thermodynamics to fractal porous media which are specified by a mass fractal dimension, a surface fractal dimension, and a resolution length-scale. Kumar et al. (2018) studied the propagation of Rayleigh waves in isotropic homogeneous thermoelastic half-space with a double porosity structure whose surface is subjected to stress-free and thermally insulated isothermal boundary conditions. Isean (1986) developed a linear theory of thermoelastic materials with voids. He examined the acceleration waves, a few equilibrium problems, and some general theorems (such as uniqueness, reciprocal, and variational theorems) in this theory. Singh et al. (2020) studied the propagation of time-harmonic plane waves in an infinite thermoelastic solid medium with double porosity.

The literature on thermal effects in continuum mechanics uses a variety of parabolic and hyperbolic ideas to explain heat conduction. The conventional thermoelasticity theory, based on the classical Fourier law of heat conduction, suffers from the deficiency of admitting thermal signals propagating with infinite speed, which is physically unrealistic. The conventional thermoelasticity theories have been generalized to remove this physically unrealistic phenomenon. The hyperbolic type thermoelasticity (nonconventional thermoelasticity) theories removed the unrealistic phenomena because, in hyperbolic type problems, the flow of heat is modelled with a finite speed of thermal signals and thermoelasticity theories admitting such signals are traditionally called thermoelasticity theories with second sound. Contributions to the theory of thermoelasticity with thermal relaxation and the temperature-rate-dependent thermoelasticity

theory are reviewed in Chandrasekharaiah (1998).

Lord and Shulman (1967) formulated a generalized theory of thermoelasticity that is based on the heat conduction equation of Maxwell and Cattaneo-Vernotte (CV). This generalized thermoelasticity theory introduced one relaxation time and a parabolic type heat conduction equation changed into a hyperbolic type equation, which is often named the LS model and broadly used in cases of low temperature and heat flux. Green and Lindsay (1972) developed a theory referred to as GL theory, which involves two relaxation times. Green and Naghdi (1992, 1993) introduced three models of generalized thermoelasticity of homogeneous isotropic materials, which are known as models of type-I, II, and III, respectively.

The next generalized thermoelasticity theory is referred to as the dual-phase-lag model (DPL) proposed by Tzou. Tzou (1995) considered a constitutive equation to describe the lagging behavior due to heat flux  $(\tau_q)$  and temperature gradient  $(\tau_T)$  in the heat conduction in thermoelastic solids. The delay time  $\tau_q$  is interpreted as the relaxation time due to the fasttransient effects of thermal inertia (or small-scale effects of heat transport in time), and is called the phase-lag of the heat flux. The other delay time  $\tau_T$  is interpreted as that caused by the microstructural interactions (small-scale heat transport mechanisms occurring in microscale or small-scale effects of heat transport in space). It is known as the phase-lag of the temperature gradient and is related to processes like phonon-electron interaction or phonon scattering. The two phase-lags are regarded as the material's inherent structural or thermal characteristics. Mittal and Kulkarni (2018) discussed a dual-phase-lag model using the fractional theory of thermoelasticity with relaxation time. A three-phase-lag model of the linearised theory of coupled thermoelasticity was developed by Roy Choudhuri (2007) by taking into account the heat conduction law, which takes into account the thermal displacement gradient and temperature gradient among the constitutive factors. In this model, the Fourier law is modified with three different translations for the heat flux vector, the temperature gradient, and the thermal displacement gradient. This model is an extension of the thermoelastic models developed by Lord-Shulman, Green-Naghdi, and Tzou. Abouelregal (2019) presented a revised thermoelastic model of heat conduction that builds upon the Roychoudhuri model (TPL) (Choudhuri, 2007) and incorporates a higher level of time derivative. The Taylor series expansions used in this new model, which include three distinct phase lags for the heat flux, thermal displacement, and temperature gradient, replace Fourier's equation of heat conduction.

Biswas (2020a) studied surface waves in the nonlocal thermoelastic orthotropic medium in the presence of voids. Khurana and Tomar (2016) investigated wave propagation in nonlocal microstretch solids. Pramanik and Biswas (2020) innovated surface waves in a nonlocal thermoelastic medium with the help of a state approach system. Gupta and Mukhopadhyay (2019) developed a study on generalized thermoelasticity proposition grounded on a nonlocal heat conduction model with the dual-phase-lag model. Khalili (2003) studied the coupling effects in double porosity media with the deformable matrix. Biswas and Mukhopadhyay (2017) proposed an eigenfunction expansion system to analyze thermal shock behavior in the magnetothermoelastic orthotropic medium under the three-phase-lag model. Biswas (2020b) delved Rayleigh waves in a nonlocal thermoelastic layer lying over a nonlocal thermoelastic half-space.

Kalkal et al. (2021) studied a three-phase-lag functionally graded thermoelastic model having double porosity and gravitational effect. Haque and Biswas (2021) discussed the propagation of Rayleigh waves in a nonlocal thermoelastic layer that is lying over a nonlocal thermoelastic half-space. Haque and Biswas (2024) investigated the propagation of Rayleigh waves in a nonlocal thermoelastic isotropic layer that lying over a nonlocal thermoelastic isotropic half-space in the context of the Green and Lindsay model and nonlocal elasticity theory in the presence of the void. Sherief and Saleh (2005) formulated a half-space problem in the proposition of generalized thermoelastic diffusion. Biswas (2021) investigated the thermal shock response in a homogeneous orthotropic medium under the horizon of the three-phase lag model in the presence of voids. Mondal et al. (2019) investigated waves in dual-phase-lag thermoelastic materials with voids grounded on Eringen's nonlocal elasticity. Sarkar and Tomar (2019) discovered plane waves in nonlocal thermoelastic solids with voids.

In this paper, we analyze the constitutive relations and field equations for thermoelastic solids with double porosity structure based on Eringen's nonlocal theory of elasticity in spatial form. Rayleigh wave propagation in a nonlocal isotropic medium in the presence of double voids has been investigated. The problem is treated in the context of the dual-phase-lag model. A differential equation is formed by employing normal mode analysis, which is then solved. To demonstrate and compare theoretical developments, the numerical results of stress, displacement, and temperature for local vs. nonlocal, voids vs. without voids, against time and distance are presented graphically.

## 2 Basic relations and equations

We first build constitutive relations and field equations. Let us examine a continuum thermoelastic body with double porosity, circumscribed by the surface area S and containing volume V. Consider  $\mathbf{x} = (x_1, x_2, x_3)$  be any typical point of the considered body in the reference state and  $\mathbf{x}' = (x_1, x_2, x_3)$  be any surrounding point of  $\mathbf{x}$ .

Suppose that  $T = \theta - T_0$ , where  $T_0$  is the temperature of the material in initial state such that  $\left|\frac{T}{T_0}\right| << 1$  and  $\theta$  be the absolute temperature of the material. We assume the set of basic variables at two neighboring point  $\mathbf{x}$  and  $\mathbf{x}'$  respectively, given as follows:

$$X = \{e_{ij}(\mathbf{x}), \phi(\mathbf{x}), \phi_{,i}(\mathbf{x}), \psi(\mathbf{x}), \psi_{,i}(\mathbf{x}), T(\mathbf{x})\},$$

$$X' = \{e_{ij}(\mathbf{x}'), \phi(\mathbf{x}'), \phi_{,i}(\mathbf{x}'), \psi(\mathbf{x}'), \psi_{,i}(\mathbf{x}'), T(\mathbf{x}')\}$$
(1)

where  $e_{ij} = \frac{1}{2}(u_{i,j} + u_{j,i})$ ; (i, j = 1, 2, 3) are the strain tensor within the context of linear theory,  $u_i$  are the displacement vector during deformation process,  $\phi = v_1(\mathbf{x}, t) - (v_1)_R$  and  $\psi = v_2(\mathbf{x}, t) - (v_2)_R$  are, respectively, the change in void volume fraction from the reference void volume corresponding to the first and second kind of voids. A comma (,) notation in the subscript presents the spatial derivative.

The strain energy function W for nonlocal thermoelastic materials with double voids can

be taken as:

$$2W = C_{ijkl}e_{ij}(\mathbf{x})e_{kl}(\mathbf{x}') + m\phi(\mathbf{x})\phi(\mathbf{x}') + p\psi(\mathbf{x})\psi(\mathbf{x}') + A_{ij}\phi_{,i}(\mathbf{x})\phi_{,i}(\mathbf{x}') + \gamma_{ij}\psi_{,i}(\mathbf{x})\psi_{,i}(\mathbf{x}')$$

$$+ B_{ij}[e_{ij}(\mathbf{x})\phi(\mathbf{x}') + e_{ij}(\mathbf{x}')\phi(\mathbf{x})] + L_{ij}[e_{ij}(\mathbf{x})\psi(\mathbf{x}') + e_{ij}(\mathbf{x}')\psi(\mathbf{x})] + D_{ijk}[e_{ij}(\mathbf{x})\phi_{,k}(\mathbf{x}')$$

$$+ e_{ij}(\mathbf{x}')\phi_{,k}(\mathbf{x})] + E_{ijk}[e_{ij}(\mathbf{x})\psi_{,k}(\mathbf{x}') + e_{ij}(\mathbf{x}')\psi_{,k}(\mathbf{x})] + D_{i}[\phi(\mathbf{x})\phi_{,i}(\mathbf{x}') + \phi(\mathbf{x}')\phi_{,i}(\mathbf{x})]$$

$$+ E_{i}[\psi(\mathbf{x})\psi_{,i}(\mathbf{x}') + \psi(\mathbf{x}')\psi_{,i}(\mathbf{x})] + b_{ij}[\phi_{,i}(\mathbf{x})\psi_{,j}(\mathbf{x}') + \phi_{,i}(\mathbf{x}')\psi_{,j}(\mathbf{x})] + l[\phi(\mathbf{x})\psi(\mathbf{x}')$$

$$+ \phi(\mathbf{x}')\psi(\mathbf{x})] + b_{i}[\phi(\mathbf{x})\psi_{,i}(\mathbf{x}') + \phi(\mathbf{x}')\psi_{,i}(\mathbf{x})] + d_{i}[\phi_{,i}(\mathbf{x})\psi(\mathbf{x}') + \phi_{,i}(\mathbf{x}')\psi(\mathbf{x})]$$

$$- \beta_{ij}[e_{ij}(\mathbf{x})T(\mathbf{x}') + e_{ij}(\mathbf{x}')T(\mathbf{x})] - aT(\mathbf{x})T(\mathbf{x}') - \gamma_{1}[\phi(\mathbf{x})T(\mathbf{x}') + \phi(\mathbf{x}')T(\mathbf{x})] - \gamma_{2}[\psi(\mathbf{x})T(\mathbf{x}') + \psi(\mathbf{x}')T(\mathbf{x})]$$

$$+ \psi(\mathbf{x}')T(\mathbf{x})] - a_{i}[\phi_{,i}(\mathbf{x})T(\mathbf{x}') + \phi_{,i}(\mathbf{x}')T(\mathbf{x})] - h_{i}[\psi_{,i}(\mathbf{x})T(\mathbf{x}') + \psi_{,i}(\mathbf{x}')T(\mathbf{x})],$$

where  $C_{ijkl}$ ,  $m, p, A_{ij}, \gamma_{ij}, B_{ij}, L_{ij}, D_{ijk}, E_{ijk}, D_i, E_i, b_{ij}, l, b_i, d_i, a, \gamma_1, \gamma_2, a_i$  and  $h_i$  are the constitutive coefficients and prescribed function of the positions  $\mathbf{x}$  and  $\mathbf{x}'$ 

Following Eringen (1974), the basic constitutive relations can be obtained from the following relation:

$$\Gamma = \int_{V} \left[ \frac{\partial W}{\partial X} + \left( \frac{\partial W}{\partial X'} \right)^{s} \right] dV(\mathbf{x}'), \tag{3}$$

where the superscript 's' is the symmetry of that quantity with respect to the interchange of  $\mathbf{x}$  and  $\mathbf{x}'$ .

Further, the set  $\Gamma = \{\tau_{ij}, \sigma_i, -\xi, \tau_i, -\zeta, \rho\eta\}$  is an ordered set with the set X.

Here  $\tau_{ij}$  are the stress tensor,  $\xi$  and  $\zeta$  represent the intrinsic equilibrated body force densities,  $\sigma_i$  and  $\tau_i$  denote the equilibrated stress vectors,  $\eta$  is the specific entropy.

Using (1) and (3), we derive the following:

$$\tau_{ij} = \int_{V} \left[ \frac{\partial W}{\partial e_{ij}(\mathbf{x})} + \left( \frac{\partial W}{\partial e_{ij}(\mathbf{x}')} \right)^{s} \right] dV(\mathbf{x}'), \tag{4}$$

$$\sigma_i = \int_V \left[ \frac{\partial W}{\partial \phi_{,i}(\mathbf{x})} + \left( \frac{\partial W}{\partial \phi_{,i}(\mathbf{x}')} \right)^s \right] dV(\mathbf{x}'), \tag{5}$$

$$-\xi = \int_{V} \left[ \frac{\partial W}{\partial \phi(\mathbf{x})} + \left( \frac{\partial W}{\partial \phi(\mathbf{x}')} \right)^{s} \right] dV(\mathbf{x}'), \tag{6}$$

$$\tau_{i} = \int_{V} \left[ \frac{\partial W}{\partial \psi_{,i}(\mathbf{x})} + \left( \frac{\partial W}{\partial \psi_{,i}(\mathbf{x}')} \right)^{s} \right] dV(\mathbf{x}'), \tag{7}$$

$$-\zeta = \int_{V} \left[ \frac{\partial W}{\partial \psi(\mathbf{x})} + \left( \frac{\partial W}{\partial \psi(\mathbf{x}')} \right)^{s} \right] dV(\mathbf{x}'), \tag{8}$$

$$\rho \eta = \int_{V} \left[ \frac{\partial W}{\partial T(\mathbf{x})} + \left( \frac{\partial W}{\partial T(\mathbf{x}')} \right)^{s} \right] dV(\mathbf{x}'), \tag{9}$$

Inserting (2) into (4)-(9), we obtain

$$\tau_{ij} = \int_{V} [C_{ijkl}(\mathbf{x}, \mathbf{x}')e_{kl}(\mathbf{x}') + B_{ij}(\mathbf{x}, \mathbf{x}')\phi(\mathbf{x}') + L_{ij}(\mathbf{x}, \mathbf{x}')\psi(\mathbf{x}') + D_{ijk}(\mathbf{x}, \mathbf{x}')\phi_{,k}(\mathbf{x}') + E_{ijk}(\mathbf{x}, \mathbf{x}')\psi_{,k}(\mathbf{x}') - \beta_{ij}(\mathbf{x}, \mathbf{x}')T(\mathbf{x}')]dV(\mathbf{x}'),$$
(10)

$$\sigma_{i} = \int_{V} [D_{kli}(\mathbf{x}, \mathbf{x}') e_{kl}(\mathbf{x}') + A_{ij}(\mathbf{x}, \mathbf{x}') \phi_{,j}(\mathbf{x}') + b_{ij}(\mathbf{x}, \mathbf{x}') \psi_{,j}(\mathbf{x}') + D_{i}(\mathbf{x}, \mathbf{x}') \phi(\mathbf{x}') + d_{i}(\mathbf{x}, \mathbf{x}') \psi(\mathbf{x}')] dV(\mathbf{x}'),$$
(11)

$$\xi = -\int_{V} [m(\mathbf{x}, \mathbf{x}')\phi(\mathbf{x}') + B_{ij}(\mathbf{x}, \mathbf{x}')e_{ij}(\mathbf{x}') + D_{i}(\mathbf{x}, \mathbf{x}')\phi_{,i}(\mathbf{x}') + l(\mathbf{x}, \mathbf{x}')\psi(\mathbf{x}') + b_{i}(\mathbf{x}, \mathbf{x}')\psi_{,i}(\mathbf{x}') - \gamma_{1}(\mathbf{x}, \mathbf{x}')T(\mathbf{x}')]dV(\mathbf{x}'),$$
(12)

$$\tau_{i} = \int_{V} \left[ E_{kli}(\mathbf{x}, \mathbf{x}') e_{kl}(\mathbf{x}') + \gamma_{ij}(\mathbf{x}, \mathbf{x}') \psi_{,j}(\mathbf{x}') + b_{ij}(\mathbf{x}, \mathbf{x}') \phi_{,j}(\mathbf{x}') + E_{i}(\mathbf{x}, \mathbf{x}') \psi(\mathbf{x}') + b_{ij}(\mathbf{x}, \mathbf{x}') \phi(\mathbf{x}') \right] dV(\mathbf{x}'),$$
(13)

$$\zeta = -\int_{V} [l(\mathbf{x}, \mathbf{x}')\phi(\mathbf{x}') + L_{ij}(\mathbf{x}, \mathbf{x}')e_{ij}(\mathbf{x}') + E_{i}(\mathbf{x}, \mathbf{x}')\psi_{,i}(\mathbf{x}') + p(\mathbf{x}, \mathbf{x}')\psi(\mathbf{x}') + d_{i}(\mathbf{x}, \mathbf{x}')\phi_{,i}(\mathbf{x}') - \gamma_{2}(\mathbf{x}, \mathbf{x}')T(\mathbf{x}')]dV(\mathbf{x}'),$$
(14)

$$\rho \eta = \int_{V} [\beta_{ij}(\mathbf{x}, \mathbf{x}') e_{ij}(\mathbf{x}') + a(\mathbf{x}, \mathbf{x}') T(\mathbf{x}') + \gamma_{1}(\mathbf{x}, \mathbf{x}') \phi(\mathbf{x}') + \gamma_{2}(\mathbf{x}, \mathbf{x}') \psi(\mathbf{x}') + a_{i}(\mathbf{x}, \mathbf{x}') \phi_{,i}(\mathbf{x}') + h_{i}(\mathbf{x}, \mathbf{x}') \psi_{,i}(\mathbf{x}')] dV(\mathbf{x}').$$
(15)

For centro-symmetric, isotropic material, the constitutive coefficients are given by

$$D_{ijk} = E_{ijk} = D_i = E_i = d_i = b_i = a_i = h_i = 0$$

$$C_{ijkl}(\mathbf{x}, \mathbf{x}') = \lambda(\mathbf{x}, \mathbf{x}')\delta_{ij}\delta_{kl} + 2\mu(\mathbf{x}, \mathbf{x}')\delta_{ik}\delta_{jl}$$

$$\{A_{ij}, B_{ij}, b_{ij}, \gamma_{ij}, L_{ij}, \beta_{ij}\}(\mathbf{x}, \mathbf{x}') = \{\alpha, h, b_1, \gamma, d, \beta\}(\mathbf{x}, \mathbf{x}')\delta_{ij}$$

where  $\lambda$  and  $\mu$  are the Lamé's constants, the quantities  $\alpha, h, b_1, \gamma, d, \gamma_1, \gamma_2$  and a are constitutive coefficients. All the constitutive coefficients are functions of  $|\mathbf{x} - \mathbf{x}'|$  and attenuate with distance because for most of the materials cohesive zone is very small. Within the cohesive zone, the intermolecular forces drop significantly with the distance from the reference point, i.e.,

$$\lim_{(|\mathbf{x} - \mathbf{x}'|) \to \infty} \lambda(|\mathbf{x} - \mathbf{x}'|) \to 0$$

etc.

Thus constitutive relations (10)-(15) become

$$\tau_{ij} = \int_{V} [\lambda(|\mathbf{x} - \mathbf{x}'|)\delta_{ij}e_{kk}(\mathbf{x}') + 2\mu(|\mathbf{x} - \mathbf{x}'|)e_{ij}(\mathbf{x}') + h(|\mathbf{x} - \mathbf{x}'|)\delta_{ij}\phi(\mathbf{x}') + d(|\mathbf{x} - \mathbf{x}'|)\delta_{ij}\psi(\mathbf{x}') - \beta(|\mathbf{x} - \mathbf{x}'|)\delta_{ij}T(\mathbf{x}')]dV(\mathbf{x}'),$$
(16)

$$\sigma_i = \int_V [\alpha(|\mathbf{x} - \mathbf{x}'|)\phi_{,i}(\mathbf{x}') + b_1(|\mathbf{x} - \mathbf{x}'|)\psi_{,i}(\mathbf{x}')]dV(\mathbf{x}'), \tag{17}$$

$$\xi = -\int_{V} [m(|\mathbf{x} - \mathbf{x}'|)\phi(\mathbf{x}') + h(|\mathbf{x} - \mathbf{x}'|)e_{ii}(\mathbf{x}') + l(|\mathbf{x} - \mathbf{x}'|)\psi(\mathbf{x}') - \gamma_{1}(|\mathbf{x} - \mathbf{x}'|)T(\mathbf{x}')]dV(\mathbf{x}'),$$
(18)

$$\tau_{i} = \int_{V} [b_{1}(|\mathbf{x} - \mathbf{x}'|)\phi_{,i}(\mathbf{x}') + \gamma(|\mathbf{x} - \mathbf{x}'|)\psi_{,i}(\mathbf{x}')]dV(\mathbf{x}'), \tag{19}$$

$$\zeta = -\int_{V} [l(|\mathbf{x} - \mathbf{x}'|)\phi(\mathbf{x}') + d(|\mathbf{x} - \mathbf{x}'|)e_{ii}(\mathbf{x}') + p(|\mathbf{x} - \mathbf{x}'|)\psi(\mathbf{x}') - \gamma_{2}(|\mathbf{x} - \mathbf{x}'|)T(\mathbf{x}')]dV(\mathbf{x}'),$$
(20)

$$\rho \eta = \int_{V} [\beta(|\mathbf{x} - \mathbf{x}'|)e_{ii}(\mathbf{x}') + a(|\mathbf{x} - \mathbf{x}'|)T(\mathbf{x}') + \gamma_{1}(|\mathbf{x} - \mathbf{x}'|)\phi(\mathbf{x}') - \gamma_{2}(|\mathbf{x} - \mathbf{x}'|)\psi(\mathbf{x}')]dV(\mathbf{x}').$$
(21)

We assume that all the constitutive coefficients attenuate with the same degree and attain their maxima at  $\mathbf{x} = \mathbf{x}'$ . The nonlocal coefficients (with unprimed notations) and local elastic coefficients have the following relations (with primed notations) as:

$$\{\lambda, \mu, h, d, \alpha, \gamma, m, p, l, b_1, a, \gamma_1, \gamma_2\} = \{\lambda', \mu', h', d', \alpha', \gamma', m', p', l', b'_1, a', \gamma'_1, \gamma'_2, \}G(|\mathbf{x} - \mathbf{x}'|, \Xi),$$

$$(22)$$

where  $G(|\mathbf{x} - \mathbf{x}'|, \Xi)$  is a nonlocal kernel expressing the effect of remote point  $\mathbf{x}'$  to the point  $\mathbf{x}$ . The parameter  $\Xi = \frac{\varepsilon}{\Theta}$  is nonlocal parameter, where  $\varepsilon = e_0 a_{cl}$ ,  $a_{cl}$  being the internal characteristic length,  $\Theta$  is the external characteristic length,  $e_0$  is a material constant.

The nonlocal kernel function has the following properties:

- (i)  $\int_V G(|\mathbf{x} \mathbf{x}'|, \Xi)]dV(\mathbf{x}') = 1.$
- (ii) The function G attains its peak at  $(|\mathbf{x} \mathbf{x}'| = 0)$  and generally decays with decreasing  $(|\mathbf{x} \mathbf{x}'|)$ .
  - (iii) Following Eringen (1974), we have

$$(1 - \varepsilon^2 \nabla^2) G(|\mathbf{x} - \mathbf{x}'|, \Xi) = \delta(|\mathbf{x} - \mathbf{x}'|), \tag{23}$$

where  $\nabla^2 = \frac{\partial^2}{\partial x^2} + \frac{\partial^2}{\partial z^2}$ .

Operating  $(1 - \varepsilon^2 \nabla^2)$  on the equations (16)-(21) and employing (22) and (23) we get the constitutive relations for a uniform nonlocal isotropic thermoelastic material possessing double porosity structure as follows:

$$(1 - \varepsilon^2 \nabla^2) \tau_{ij} = \lambda' \delta_{ij} e_{kk}(\mathbf{x}) + 2\mu' e_{ij}(\mathbf{x}) + h' \delta_{ij} \phi(\mathbf{x}) + d' \delta_{ij} \psi(\mathbf{x}) - \beta' \delta_{ij} T(\mathbf{x}), \tag{24}$$

$$(1 - \varepsilon^2 \nabla^2) \sigma_i = \alpha' \phi_{,i}(\mathbf{x}) + b_1' \psi_{,i}(\mathbf{x}), \tag{25}$$

$$(1 - \varepsilon^2 \nabla^2) \xi = -m' \phi(\mathbf{x}) - h' e_{ii}(\mathbf{x}) - l' \psi(x) + \gamma_1' T(\mathbf{x}), \tag{26}$$

$$(1 - \varepsilon^2 \nabla^2) \tau_i = b_1' \phi_{,i}(\mathbf{x}) + \gamma' \psi_{,i}(\mathbf{x}), \tag{27}$$

$$(1 - \varepsilon^2 \nabla^2) \zeta = -l' \phi(\mathbf{x}) - d' e_{ii}(\mathbf{x}) - p' \psi(x) + \gamma_2' T(\mathbf{x}), \tag{28}$$

$$(1 - \varepsilon^2 \nabla^2 \rho \eta = \beta' e_{ii}(\mathbf{x}) + \gamma_1' \phi(\mathbf{x}) + \gamma_2' \psi(\mathbf{x}) + a' T(\mathbf{x}).$$
(29)

Here, we have used the following property of Dirac delta function:

$$\int f(x)\delta(x-a)dx = f(a)$$

We propose an Eringen-type (1974) Fourier law for the nonlocal generalization of the dual-

phase-lag model (Tzou (1995)) as

$$(1 - \varepsilon^2 \nabla^2) \left( 1 + \tau_q \frac{\partial}{\partial t} \right) q_i = -K \left( 1 + \tau_T \frac{\partial}{\partial t} \right) T_{,i}(\mathbf{x}), \tag{30}$$

$$(1 - \varepsilon^2 \nabla^2) \rho \eta = \beta' e_{ii}(\mathbf{x}) + \gamma_1' \phi(\mathbf{x}) + \gamma_2' \psi(\mathbf{x}) + a' T(\mathbf{x}). \tag{31}$$

The energy equation is

$$q_{i,i} = -\rho T_0 \dot{\eta}. \tag{32}$$

Operating  $(1 - \varepsilon^2 \nabla^2)$  on the equation (32) and using (30) and (31) we get

$$K\left(1 + \tau_T \frac{\partial}{\partial t}\right) T_{,ii}(\mathbf{x}) = \left(1 + \tau_q \frac{\partial}{\partial t}\right) \left(\beta' T_0 \dot{e}_{ii}(\mathbf{x}) + \gamma_1' T_0 \dot{\phi}(\mathbf{x}) + \gamma_2' T_0 \dot{\psi}(\mathbf{x}) + \rho C_v \dot{T}(\mathbf{x})\right), \quad (33)$$

where K is the thermal conductivity of the material,  $\tau_T$  and  $\tau_q$  are phase lags due to the temperature gradient and heat flux vector respectively,  $q_i$  are the components of the heat flux vector and  $aT_0 = \rho C_v$  and  $C_v$  is the specific heat at constant strain.

For the strain energy density function to be positive definite, the following inequalities must hold:

$$\mu > 0, 3\lambda + 2\mu > 0, p > 0, mp - l^2 > 0, \alpha > 0, \alpha \gamma > b_1^2,$$
  
 $(3\lambda + 2\mu)(mp - l^2) > 3(md^2 + pb^2 - 2lbd)$  (Biswas and Mahato (2024a, 2024b)).

The equations of small motion for a uniform nonlocal thermoelastic material with double void parameters are given (Isean and Quintanilla (2014)) as follows:

Stress equations of motion:

$$\tau_{ij,j} + \rho f_i = \rho \ddot{u}_i, \tag{34}$$

Equilibrated stress equations of motion:

$$\sigma_{j,j} + \xi + \rho g = \chi_1 \ddot{\phi},\tag{35}$$

$$\tau_{j,j} + \zeta + \rho \bar{l} = \chi_2 \ddot{\psi},\tag{36}$$

where (i,j=1,2,3);  $f_i$  is the body force density,  $\chi_1$  and  $\chi_2$  are the equilibrated inertia per unit mass per unit volume corresponding to the first and second kind of voids respectively, g and  $\bar{l}$  are the corresponding extrinsic equilibrated body forces per unit mass corresponding to the first and second type of voids respectively, and  $\rho$  is the mass density.

Using the equations (24)-(28) in the equations (34)-(36) and omitting prime  $(\prime)$  from the constitutive coefficients, we obtain the governing equations in a homogeneous isotropic nonlocal thermoelastic material with double porosity structure without body forces, extrinsic equili-

brated body forces and heat sources as follows:

$$\mu \nabla^2 \mathbf{u} + (\lambda + \mu) \nabla (\nabla \cdot \mathbf{u}) + h \nabla \phi + d \nabla \psi - \beta \nabla T = (1 - \varepsilon^2 \nabla^2) \rho \ddot{\mathbf{u}}, \tag{37}$$

$$\alpha \nabla^2 \phi + b_1 \nabla^2 \psi - h \nabla \cdot \mathbf{u} - m\phi - l\psi + \gamma_1 T = (1 - \varepsilon^2 \nabla^2) \chi_1 \ddot{\phi}, \tag{38}$$

$$b_1 \nabla^2 \phi + \gamma \nabla^2 \psi - d\nabla \cdot \mathbf{u} - l\phi - p\psi + \gamma_2 T = (1 - \varepsilon^2 \nabla^2) \chi_2 \ddot{\psi}, \tag{39}$$

$$K\left(1 + \tau_T \frac{\partial}{\partial t}\right) \nabla^2 T = \left(1 + \tau_q \frac{\partial}{\partial t}\right) \left(\beta T_0 \nabla \cdot \dot{\mathbf{u}} + \gamma_1 T_0 \dot{\phi} + \gamma_2 T_0 \dot{\psi} + \rho C_v \dot{T}\right),\tag{40}$$

where  $\mathbf{u} = (u, 0, w)$  is the displacement vector in nonlocal isotropic thermoelastic medium.

The coefficients h and d represent the coupling of void volume fractions of each type of voids with the normal stress. The gradient of void volume fractions  $\phi$  and  $\psi$  is coupled by the parameters  $\alpha$  and  $\gamma$  to the associated equilibrated stress vectors that correspond to the first type of voids  $\sigma_i$  and the second kind of voids  $\tau_i$ . The parameters  $b_1$  acts as a cross-coupling between the gradient of both void volume fractions and equilibrated stresses. The parameter m and p couple the void volume fractions  $\phi$  and  $\psi$  with the intrinsic equilibrated body force densities  $\xi$  and  $\zeta$  respectively, also l acts as a cross-coupling between void volume fractions and the intrinsic equilibrated body force densities,  $\gamma_1$  and  $\gamma_2$  are the thermo-void coefficients of first kind of voids and second kind of voids respectively.

## 3 Solution of the problem:

To solve the equations (37)-(40), we employ normal mode analysis and consider the solution as given below:

$$(u, w, \phi, \psi, T)(x, z, t) = (\bar{u}, \bar{w}, \bar{\phi}, \bar{\psi}, \bar{T})(z) \exp[ik(x - ct)], \tag{41}$$

where  $\bar{u}, \bar{w}, \bar{\phi}, \bar{\psi}$  and  $\bar{T}$  are the amplitudes of the physical quantities, k is the wave number, c is the phase velocity in the direction of x-axis. With the help of the equation (41), equations (37)-(40) reduce to the following forms:

$$(D^2 + a_1)\bar{u} + a_2D\bar{w} + a_3\bar{\phi} + a_4\bar{\psi} + a_5\bar{T} = 0, \tag{42}$$

$$a_7 D\bar{u} + (D^2 + a_6)\bar{w} + a_8 D\bar{\phi} + a_9 D\bar{\psi} + a_{10} D\bar{T} = 0, \tag{43}$$

$$a_{15}\bar{u} + a_{12}D\bar{w} + (D^2 + a_{11})\bar{\phi} + (a_{13}D^2 + a_{14})\bar{\psi} + a_{16}\bar{T} = 0,$$
 (44)

$$a_{19}\bar{u} + a_{20}D\bar{w} + (a_{17}D^2 + a_{18})\bar{\phi} + (D^2 + a_{21})\bar{\psi} + a_{22}\bar{T} = 0,$$
 (45)

$$a_{24}\bar{u} + a_{23}D\bar{w} + a_{26}\bar{\phi} + a_{27}\bar{\psi} + (D^2 + a_{25})\bar{T} = 0,$$
 (46)

The condition for the existence of a non-trivial solution of the system of homogeneous

equations (42)-(46) provides the following tenth-order differential equation:

$$[D^{10} + N_1 D^8 + N_2 D^6 + N_3 D^4 + N_4 D^2 + N_5](\bar{u}, \bar{w}, \bar{\phi}, \bar{\psi}, \bar{T})(z) = 0, \tag{47}$$

where  $D \equiv \frac{d}{dz}$ ,  $a_1, a_2, a_3, ..., a_{25}$ , and  $N_n(n = 1, 2, 3, 4, 5)$  are provided in "**Appendix**".

## 4 Solution of the differential equation

Assuming the regularity condition at infinity, the solution of Eqn. (47) is obtained as

$$(\bar{u}, \bar{w}, \bar{\phi}, \bar{\psi}, \bar{T})(z) = \sum_{n=1}^{5} (h_n, B_n, C_n, D_n, E_n) exp[-\lambda_n z].$$
(48)

Inserting Eqn. (48) into the equations (42)-(46), we obtain the following relations:

$$B_n = x_n h_n, C_n = y_n h_n, D_n = z_n h_n, E_n = e_n h_n.$$

From Eqn. (41) the displacement components, void volume fractions, and temperature are obtained as:

$$u = \sum_{n=1}^{5} h_n exp[-\lambda_n z + ik(x - ct)], \tag{49}$$

$$w = \sum_{n=1}^{5} B_n exp[-\lambda_n z + ik(x - ct)],$$
 (50)

$$\phi = \sum_{n=1}^{5} C_n exp[-\lambda_n z + ik(x - ct)], \tag{51}$$

$$\psi = \sum_{n=1}^{5} D_n exp[-\lambda_n z + ik(x - ct)], \tag{52}$$

$$T = \sum_{n=1}^{5} E_n exp[-\lambda_n z + ik(x - ct)].$$

$$(53)$$

The stress components are obtained as:

$$\tau_{xx}^{L} = (\lambda + 2\mu) \frac{\partial u}{\partial x} + \lambda \frac{\partial w}{\partial z} + h\phi + d\psi - \beta T$$

$$= \sum_{n=1}^{5} [ik(\lambda + 2\mu) - \lambda \lambda_n x_n + hy_n + dz_n - \beta e_n] h_n exp[-\lambda_n z + ik(x - ct)],$$
(54)

$$\tau_{zz}^{L} = (\lambda + 2\mu) \frac{\partial w}{\partial z} + \lambda \frac{\partial u}{\partial x} + h\phi + d\psi - \beta T$$

$$= \sum_{n=1}^{5} [ik\lambda - (\lambda + 2\mu)\lambda_n x_n + hy_n + dz_n - \beta e_n] h_n exp[-\lambda_n z + ik(x - ct)],$$
(55)

$$\tau_{xz}^{L} = \mu \left( \frac{\partial u}{\partial z} + \frac{\partial w}{\partial x} \right) = \sum_{n=1}^{5} \left[ \mu \left( ikx_n - \lambda_n \right) \right] h_n exp[-\lambda_n z + ik(x - ct)]. \tag{56}$$

## 5 Boundary Conditions

We consider the following boundary conditions at z = 0 (biswas (2020b), Mahato and Biswas (2024b)):

- (1) Mechanical boundary conditions that the surface to the half-space is traction free:
- (a) Vanishing of the normal component:

$$\tau_{zz}(x,0,t) = 0,$$

$$(1 - \epsilon^2 \nabla^2) \tau_{zz}(x, 0, t) = 0,$$

which gives

$$\tau_{zz}^{L}(x,0,t) = 0. (57)$$

(b) Vanishing of the tangential component:

$$\tau_{xz}(x,0,t) = 0,$$

$$(1 - \epsilon^2 \nabla^2) \tau_{xz}(x, 0, t) = 0,$$

which gives

$$\tau_{xz}^{L}(x,0,t) = 0. (58)$$

(2) Conditions on void volume fraction fields:

(a)

$$\sigma_z(x,0,t) = 0,$$

$$(1 - \epsilon^2 \nabla^2) \sigma_z(x, 0, t) = 0,$$

which gives

$$\sigma_z^L(x,0,t) = 0. (59)$$

(b)

$$\tau_z(x,0,t) = 0,$$

$$(1 - \epsilon^2 \nabla^2) \tau_z(x, 0, t) = 0,$$

which gives

$$\tau_z^L(x, 0, t) = 0. (60)$$

(3) Thermal boundary condition:

(i) Thermally insulated surface:

$$q_z = 0,$$

$$(1 - \epsilon^2 \nabla^2) q_z = 0,$$

which gives

$$q_z^L = 0. (61)$$

(ii) Isothermal surface:

$$T(x,0,t) = 0. (62)$$

## 6 Derivation of the frequency equations:

Substituting from the expressions of considered variables into the above boundary conditions (57)-(62) we can obtain the following equations:

$$\sum_{n=1}^{5} f_n h_n = 0, (63)$$

$$\sum_{n=1}^{5} g_n h_n = 0, (64)$$

$$\sum_{n=1}^{5} l_n h_n = 0, (65)$$

$$\sum_{n=1}^{5} m_n h_n = 0, (66)$$

For thermally insulated surface,

$$\sum_{n=1}^{5} r_n h_n = 0, (67)$$

For isothermal surface,

$$\sum_{n=1}^{5} e_n h_n = 0, (68)$$

Using the above equations we derive the frequency equation of Rayleigh waves in nonlocal thermoelastic medium with double porosity under DPL model as follows:

(a) Frequency equation of Rayleigh waves for thermally insulated surface:

$$\begin{vmatrix} f_1 & f_2 & f_3 & f_4 & f_5 \\ g_1 & g_2 & g_3 & g_4 & g_5 \\ l_1 & l_2 & l_3 & l_4 & l_5 \\ m_1 & m_2 & m_3 & m_4 & m_5 \\ r_1 & r_2 & r_3 & r_4 & r_5 \end{vmatrix} = 0,$$

i.e.,

$$f_1 M_1 - f_2 M_2 + f_3 M_3 - f_4 M_4 + f_5 M_5 = 0, (69)$$

where

(b) Frequency equation of Rayleigh waves for isothermal surface:

$$\begin{vmatrix} f_1 & f_2 & f_3 & f_4 & f_5 \\ g_1 & g_2 & g_3 & g_4 & g_5 \\ l_1 & l_2 & l_3 & l_4 & l_5 \\ m_1 & m_2 & m_3 & m_4 & m_5 \\ e_1 & e_2 & e_3 & e_4 & e_5 \end{vmatrix} = 0,$$

i.e.,

$$f_1M_1' - f_2M_2' + f_3M_3' - f_4M_4' + f_5M_5' = 0, (70)$$

where

$$M_1' = \begin{vmatrix} g_2 & g_3 & g_4 & g_5 \\ l_2 & l_3 & l_4 & l_5 \\ m_2 & m_3 & m_4 & m_5 \\ e_2 & e_3 & e_4 & e_5 \end{vmatrix}, M_2' = \begin{vmatrix} g_1 & g_3 & g_4 & g_5 \\ l_1 & l_3 & l_4 & l_5 \\ m_1 & m_3 & m_4 & m_5 \\ e_1 & e_3 & e_4 & e_5 \end{vmatrix}, M_3' = \begin{vmatrix} g_1 & g_2 & g_4 & g_5 \\ l_1 & l_2 & l_4 & l_5 \\ m_1 & m_2 & m_4 & m_5 \\ e_1 & e_2 & e_4 & e_5 \end{vmatrix},$$

$$M_4' = \begin{vmatrix} g_1 & g_2 & g_3 & g_5 \\ l_1 & l_2 & l_3 & l_5 \\ m_1 & m_2 & m_3 & m_5 \\ e_1 & e_2 & e_3 & e_5 \end{vmatrix}, M_5' = \begin{vmatrix} g_1 & g_2 & g_3 & g_4 \\ l_1 & l_2 & l_3 & l_4 \\ m_1 & m_2 & m_3 & m_4 \\ e_1 & e_2 & e_3 & e_4 \end{vmatrix}.$$

## 7 Solution of the frequency equation

In general, wave number (k) and hence phase velocity (c) are complex quantities. If we take

$$c^{-1} = V^{-1} + i\omega^{-1}Q,$$

the wave number can be expressed as k = R + iQ where  $R = \frac{\omega}{V}$  in which V and Q are real. V is the propagation speed, and Q is the attenuation coefficient of Rayleigh waves.

## Specific loss

The specific loss (SL) is the ratio of energy  $(\Delta W)$  dissipated in taking specimen through cycle, to elastic energy (W) stored in a specimen when the strain is at maximum. The specific loss is the most direct way of defining internal friction for a material (Puri and Cowin (2017)). For a sinusoidal surface wave of small amplitude shows that the specific loss  $\frac{\Delta W}{W}$  equals  $4\pi$  times the absolute value of the ratio of imaginary part of k to the real part of k (Kolsky (1963)), that is

$$SL = \frac{\Delta W}{W} = 4\pi \left| \frac{Im(k)}{Re(k)} \right| = 4\pi \left| \frac{VQ}{\omega} \right|.$$

## Penetration depth

The penetration depth is defined by

$$\delta = \frac{1}{|Im(k)|} = \frac{1}{|Q|}.$$

## 8 Amplitudes of displacements, void volume fraction field and temperature

Now, we derive the formulas for displacements, temperature change functions, and void volume fraction field change functions on the surface (z = 0) for the isothermal surface during the Rayleigh wave propagation.

On (z = 0), the isothermal surface can be expressed as follows:

$$u = U^* h_1 exp(-Qx + ip), \tag{71}$$

$$w = W^* h_1 exp(-Qx + ip), \tag{72}$$

$$\phi = \Phi^* h_1 exp(-Qx + ip), \tag{73}$$

$$\psi = \Psi^* h_1 exp(-Qx + ip), \tag{74}$$

$$T = \Theta^* h_1 exp(-Qx + ip), \tag{75}$$

14

where

$$\begin{split} U^* &= f_1 + f_2\Gamma_{13} + f_3\Gamma_{14} + f_4\Gamma_{15} + f_5\Gamma_{16}, \\ W^* &= g_1 + g_2\Gamma_{13} + g_3\Gamma_{14} + g_4\Gamma_{15} + g_5\Gamma_{16}, \\ \Phi^* &= l_1 + l_2\Gamma_{13} + l_3\Gamma_{14} + l_4\Gamma_{15} + l_5\Gamma_{16}, \\ \Psi^* &= m_1 + l_2\Gamma_{13} + m_3\Gamma_{14} + 4_4\Gamma_{15} + m_5\Gamma_{16}, \\ \Theta^* &= e_1 + e_2\Gamma_{13} + e_3\Gamma_{14} + e_4\Gamma_{15} + e_5\Gamma_{16}, \\ \Gamma_1 &= m_1 - \frac{m_5}{e_5}e_1, \ \Gamma_2 &= m_2 - \frac{m_5}{e_5}e_2, \ \Gamma_3 &= m_3 - \frac{m_5}{e_5}e_3, \ \Gamma_4 &= m_4 - \frac{m_5}{e_5}e_4, \ \Gamma_5 &= \frac{e_1}{\Gamma_4}\Gamma_1 - e_1, \\ \Gamma_6 &= \frac{e_4}{\Gamma_4}\Gamma_2 - e_2, \ \Gamma_7 &= \frac{e_4}{\Gamma_4}\Gamma_3 - e_3, \ \Gamma_8 &= -\frac{\Gamma_1}{\Gamma_4}, \ \Gamma_9 &= -\frac{\Gamma_2}{\Gamma_4}, \ \Gamma_{10} &= -\frac{\Gamma_3}{\Gamma_4}, \ \Gamma_{11} &= -\frac{g_1 + g_4\Gamma_8 + g_5\Gamma_5}{g_3 + g_4\Gamma_{10} + g_5\Gamma_7}, \\ \Gamma_{12} &= -\frac{g_2 + g_4\Gamma_9 + g_5\Gamma_6}{g_3 + g_4\Gamma_{10} + g_5\Gamma_7}, \ \Gamma_{13} &= -\frac{f_1 + f_3\Gamma_{11} + f_4(\Gamma_8 + \Gamma_{10}\Gamma_{11}) + f_5(\Gamma_5 + \Gamma_7\Gamma_{11})}{f_2 + f_3\Gamma_{12} + f_4(\Gamma_9 + \Gamma_{10}\Gamma_{12}) + f_5(\Gamma_6 + \Gamma_7\Gamma_{12})}, \ \Gamma_{14} &= \Gamma_{11} + \Gamma_{12}\Gamma_{13}, \ \Gamma_{15} &= \Gamma_8 + \Gamma_{10}\Gamma_{11} + \Gamma_{13}(\Gamma_9 + \Gamma_{10}\Gamma_{12}), \ \Gamma_{16} &= \Gamma_5 + \Gamma_7\Gamma_{11} + \Gamma_{13}(\Gamma_6 + \Gamma_7\Gamma_{12}), \ p = R(x - Vt). \end{split}$$

## 9 Path of surface particles

Following Biswas (2020b), we now discuss the motion of the surface (z=0) particles of the modified Rayleigh waves. It is also revealed that when thermomechanical coupling and interaction of different fields are operative, the amplitude and slowness of the waves are no longer real. This means that the wave is damped and the phase difference exists between u and w. Therefore, on the surface (z=0), Eqs. (71) and (72) on retaining real parts lead to

$$u = |U^*|H\cos(p + \theta_1), w = |W^*|H\cos(p + \theta_2), \tag{76}$$

where  $H = h_1 exp(-Qx)$ ,  $(\theta_1, \theta_2) = (\arg(U^*), \arg(W^*))$ .

Eliminating p from the above equations, we get

$$\left(\frac{u}{|U^*|}\right)^2 - 2\left(\frac{u}{|U^*|}\right)\left(\frac{w}{|W^*|}\right)\cos(\theta_1 - \theta_2) + \left(\frac{w}{|W^*|}\right)^2 = H^2\sin^2(\theta_1 - \theta_2), \tag{77}$$

Here  $\frac{\cos^2(\theta_1 - \theta_2)}{|U^*|^2|W^*|^2} - \frac{1}{|U^*|^2|W^*|^2} = -\frac{1}{|U^*|^2|W^*|^2} \sin^2(\theta_1 - \theta_2) < 0.$ 

Therefore, Eq. (77) represents an ellipse in the x-z plane. The squares of the semi-major axis(A), semi-minor axis(B) and eccentricity (e) of the elliptical paths are given by

$$A^{2} = \frac{H^{2}}{2} \left[ |U^{*}|^{2} + |W^{*}|^{2} + ((|U^{*}|^{2} - |W^{*}|^{2})^{2} + 4|U^{*}|^{2}|W^{*}|^{2}\cos^{2}(\theta_{1} - \theta_{2}))^{\frac{1}{2}} \right]$$

$$B^{2} = \frac{H^{2}}{2} \left[ |U^{*}|^{2} + |W^{*}|^{2} - ((|U^{*}|^{2} - |W^{*}|^{2})^{2} + 4|U^{*}|^{2}|W^{*}|^{2}\cos^{2}(\theta_{1} - \theta_{2}))^{\frac{1}{2}} \right],$$

$$(78)$$

$$e^{2} = \frac{2\left[\left(|U^{*}|^{2} - |W^{*}|^{2}\right)^{2} + 4|U^{*}|^{2}|W^{*}|^{2}\cos^{2}(\theta_{1} - \theta_{2})\right]^{\frac{1}{2}}}{|U^{*}|^{2} + |W^{*}|^{2} + \left[\left(|U^{*}|^{2} - |W^{*}|^{2}\right)^{2} + 4|U^{*}|^{2}|W^{*}|^{2}\cos^{2}(\theta_{1} - \theta_{2})\right]^{\frac{1}{2}}}.$$

If  $\bar{\delta}$  is the inclination of the major axis to the wave normal then

$$\tan(2\bar{\delta}) = \frac{2\{(\tan^2\theta - 1)|U^*||W^*|\cos(\theta_1 - \theta_2) - (|U^*|^2 - |W^*|^2)\tan\theta\}}{(\tan^2\theta - 1)(|U^*|^2 - |W^*|^2) + 4|U^*||W^*|\cos(\theta_1 - \theta_2)},\tag{79}$$

where  $\theta$  represents the wave's angle of incidence.

When  $\theta = \frac{\pi}{2}$  i.e., in the case when Rayleigh wave propagation along x-axis then

$$\bar{\delta} = \frac{1}{2} \arctan\left(\frac{2|U^*||W^*|\cos(\theta_1 - \theta_2)}{|U^*|^2 - |W^*|^2}\right). \tag{80}$$

From Equation (80) it is clear that in case when the wave normal and major axis are inclined at  $\frac{\pi}{4}$  to each other so that  $\bar{\delta} = \frac{\pi}{4}$ , the horizontal and vertical displacements have equal magnitudes  $|U^*| = |W^*|$ . Thus, it can be followed that the surface particles trace elliptical paths given by Equation (77) in vertical planes parallel to the direction of wave propagation. The semi-axes depend upon  $H = h_1 exp(-Qx)$  and hence increase or decrease exponentially.

However, for  $\theta_1 - \theta_2 = \frac{\pi}{2}$  both A and B have the same sign and therefore, the surface particles trace elliptical paths in a retrograde fashion in the case. Moreover, the particle paths generate straight lines when  $\theta_1 = \theta_2$ , i.e., there is no phase difference between the functions  $U^*$  and  $W^*$ , where the incidence angle is  $\theta$ . When a Rayleigh surface wave travels into a solid, its constituent particles follow elliptical paths. The primary axis of the ellipse is perpendicular to the solid's surface, and the elliptical path's distance reduces as the wave travels deeper into the solid.

## 10 Limiting and particular cases

In this section, we derive some limiting and particular cases by considering different particular values of the parameters:

- Lord Shulman (LS) model: If we set,  $\tau_T = 0$  then we derive the Lord Shulman model.
- Coupled thermoelasticity (CT) model: If we consider  $\tau_q = \tau_T == 0$  then the present problem reduces to the case of the classical coupled thermoelasticity model.
- Nonlocal elastic medium with double voids: when thermoelastic coupling constants are absent i.e.,  $\beta = \gamma_1 = \gamma_2 = a = K = 0$  then the present study reduces to the nonlocal elastic medium with double void and the paper agrees with Kumar et al. (2021) under some suitable consideration.
- Local thermoelastic medium with double void parameters: If we ignore nonlocal parameters in governing equations and constitutive relations i.e.  $\varepsilon = 0$  then, the present study reduces to a local thermoelastic medium with double voids and without diffusion and agrees with Iesan and Quintanilla (2014), and Chirita and Arusoaie (2021) under suitable modification.
- Nonlocal thermoelastic medium without double void parameters: when void parameters are absent i.e.,  $h=d=\alpha=b_1=m=l=\gamma=\gamma_1=\gamma_2=p=\chi_1=$

 $\chi_2 = 0$  then the present study reduces to the nonlocal elastic medium without double void.

- Nonlocal elastic medium without double void: when thermoelastic coupling constants along with void parameters are absent i.e.,  $\beta = \gamma_1 = \gamma_2 = a = K = 0$  and  $h = d = \alpha = b_1 = m = l = \gamma = p = \chi_1 = \chi_2 = 0$  then the present study reduces to the nonlocal elastic medium without double void.
- Local thermoelastic medium without double voids: when void and nonlocal parameters are absent i.e.,  $h=d=\alpha=b_1=m=l=\gamma=\gamma=\gamma_1=\gamma_2=p=\chi_1=\chi_2=0$  and  $\varepsilon=0$  then the present study reduces to the local elastic medium without double void.
- Local elastic medium without double void parameters: when thermoelastic coupling constants along with nonlocal and void parameters are absent i.e.,  $\beta = \gamma_1 = \gamma_2 = a = K = 0$ ,  $\varepsilon = 0$  and  $h = d = \alpha = b_1 = m = l = \gamma = p = \chi_1 = \chi_2 = 0$  then the present study reduces to the local elastic medium without double void.

#### 11 Numerical results and discussion:

For numerical computations, we consider the following physical data of copper material, which is given by Sherief et al. (2005), Mahato and Biswas (2024b) as

$$\lambda = 7.76 \times 10^{10} \mathrm{Nm^{-2}}, \ \mu = 3.86 \times 10^{10} \mathrm{Nm^{-2}}, \ C_v = 3.831 \times 10^{3} \mathrm{m^{2} s^{-2} K^{-1}}, \ K = 3.86 \times 10^{3} \mathrm{Ns^{-1} K^{-1}}, \rho = 8.954 \times 10^{3} \mathrm{kgm^{-3}}, \ T_0 = 293 \mathrm{K}, \ \alpha_t = 1.78 \times 10^{-5} \mathrm{K^{-1}}, \ t = 1 \mathrm{s}.$$

Following Khalili, (2003) the double porous parameters are taken as,

 $h = 0.9 \times 10^{10} \mathrm{Nm^{-2}}, \ d = 0.1 \times 10^{10} \mathrm{Nm^{-2}}, \ \alpha = 1.3 \times 10^{-5} \mathrm{N}, \ b_1 = 0.12 \times 10^{-5} \mathrm{N}, \ \gamma = 1.1 \times 10^{-5} \mathrm{N}, \ \gamma_1 = 0.16 \times 10^{5} \mathrm{Nm^{-2}}, \ \gamma_2 = 0.219 \times 10^{5} \mathrm{Nm^{-2}}, \ p = 2.4 \times 10^{10} \mathrm{Nm^{-2}}, \ l = 2.5 \times 10^{10} \mathrm{Nm^{-2}}, \ m = 2.3 \times 10^{10} \mathrm{Nm^{-2}}, \ \chi_1 = 0.1456 \times 10^{-12} \mathrm{Nm^{-2} s^2}, \ \chi_2 = 0.1546 \times 10^{-12} \mathrm{Nm^{-2} s^2}.$ 

Again in order to study the numerical computation, we take  $\theta_0 = 100$ , b = 0.1m, k = 1.2m<sup>-1</sup>,  $\tau_q = 2 \times 10^{-7}$ s,  $\tau_T = 1.5 \times 10^{-7}$ s,  $\varepsilon = 0.009$  (for nonlocal case) and  $\varepsilon = 0$  (for local case).

In figures 1-8 we perform the graphs for propagation speed, attenuation coefficients, penetration depth and specific loss with respect to wave number (k) for dual-phase-lag (DPL) and Lord-Shulman (LS) models for isothermal surfaces.

Figure 1 illustrates the variation of propagation speed (V) with respect to wave number (k) for the isothermal surface. The propagation speed gradually diminishes for the presence of nonlocal parameters, and for the local parameters, it is initially showing a sudden decrease for 100 < k < 300 and a gradual decrease for 300 < k < 900. Here the propagation speed is smaller in the presence of nonlocal parameters for both the dual-phase-lag (DPL) model and Lord-Shulman (LS) model. There's a gradual decrease in propagation speed (V) for the LS model in comparison with the DPL model with the increase of wave number (k).

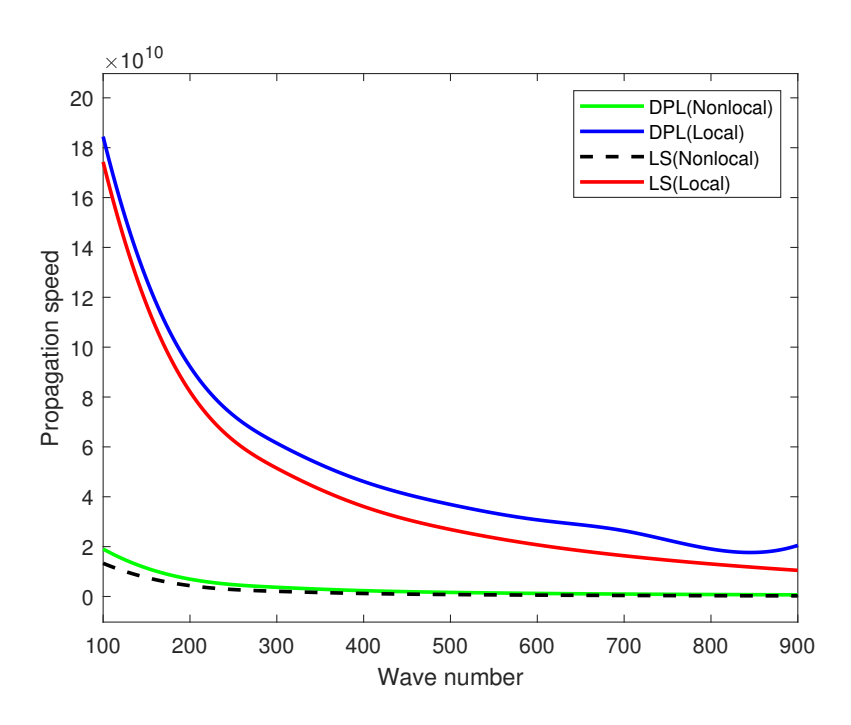


Figure 1: Propagation speed (V) against wave number (k) (for isothermal surface)

The attenuation coefficient (Q) variation for an isothermal surface with respect to wave number (k) is shown in Figure 2. Wave number (k) increases cause a progressive increase in the attenuation coefficient (Q). The attenuation coefficient (Q) for the dual-phase-lag (DPL) and Lord-Shulman (LS) models is reduced when local factors are present. When wave number (k) increases, the attenuation coefficient (Q) for the LS model gradually rises in contrast to the DPL model.

Figure 3 illustrates the variation of penetration depth  $(\delta)$  with respect to wave number (k) for the isothermal surface. When nonlocal parameters are included, the penetration depth  $(\delta)$  steadily decreases; when local parameters are present, the initial reduction is abrupt for 100 < k < 300 and gradual for 300 < k < 900. In this case, the penetration depth  $(\delta)$  for the Lord-Shulman (LS) and dual-phase-lag (DPL) models is smaller when nonlocal parameters are present. As wave number (k) increases, the penetration depth  $(\delta)$  for the LS model gradually decreases in comparison to the DPL model.

Figure 4 illustrates the variation of specific loss (SL) with respect to wave number (k) for isothermal surfaces. Here specific loss (SL) gradually increases for the nonlocal dual-phase-lag (DPL) model and it is almost constant for the nonlocal Lord-Shulman (LS) model. The specific loss (SL) for the dual-phase-lag (DPL) and Lord-Shulman (LS) models is reduced when local factors are present. The difference of specific loss (SL) between DPL (nonlocal) and LS (nonlocal) is greater with respect to the difference of specific loss (SL) between DPL (local) and Ls (local).

Figure 5 illustrates the variation of propagation speed (V) with respect to wave number (k) for the isothermal surface. The propagation (V) speed gradually diminishes for the presence

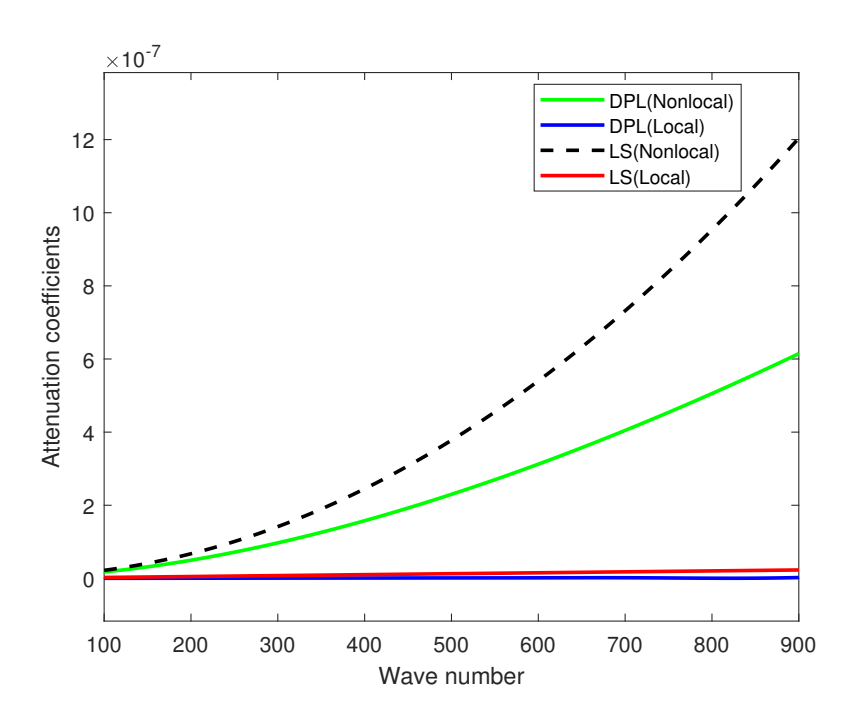


Figure 2: Attenuation coefficient (Q) against wave number (k) (for isothermal surface)

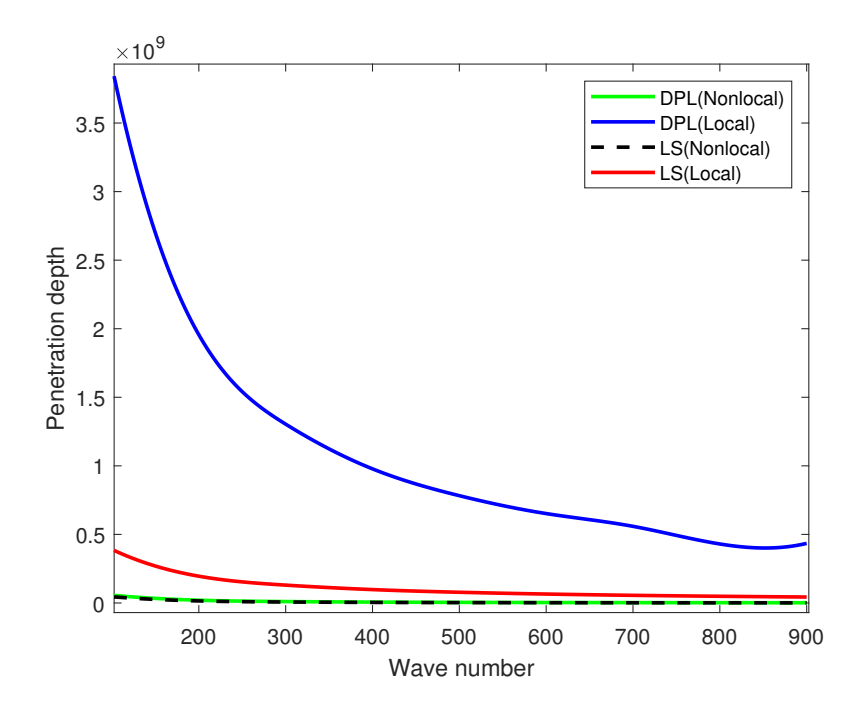


Figure 3: Penetration depth  $(\delta)$  against wave number (k) (for isothermal surface)

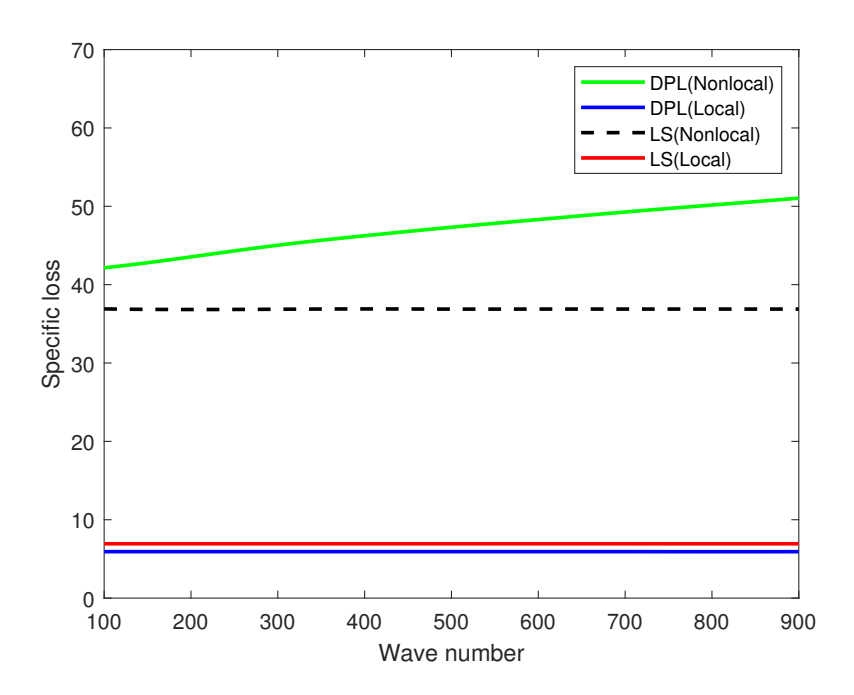


Figure 4: Specific loss (SL) against wave number (k) (for isothermal surface)

of void parameters and for the absence of void parameters it initially shows a sudden decrease for 100 < k < 300 and a gradual decrease for 300 < k < 900. Here the propagation speed is smaller in the presence of void parameters for both the models dual-phase-lag (DPL) model and Lord-Shulman (LS) model. There's a gradual decrease in propagation speed (V) for the LS model in comparison with the DPL model with the increase of wave number (k).

The attenuation coefficient (Q) variation for an isothermal surface with respect to wave number (k) is shown in Figure 6. Wave number (k) increases cause a progressive increase in the attenuation coefficient (Q). The attenuation coefficient (Q) for the dual-phase-lag (DPL) and Lord-Shulman (LS) models is reduced when void parameters are not present. When wave number (k) increases, the attenuation coefficient (Q) for the LS model gradually rises in contrast to the DPL model.

Figure 7 illustrates the variation of penetration depth  $(\delta)$  with respect to wave number (k) for the isothermal surface. When void parameters are included, the penetration depth  $(\delta)$  steadily decreases. In this case, the penetration depth  $(\delta)$  for the Lord-Shulman (LS) and dual-phase-lag (DPL) models is smaller when void parameters are present. When void parameters are present, the penetration depth  $(\delta)$  for the DPL model is higher than for the LS model. When void parameters are absent, the penetration depth  $(\delta)$  for the DPL model gradually drops for 100 < k < 700, at which point it begins to exhibit wave characteristics. Similarly, for the LS model, in the absence of void parameters, the penetration depth  $(\delta)$  also exhibits wave characteristics.

Figure 8 illustrates the variation of specific loss (SL) with respect to wave number (k) for the isothermal surface. Here specific loss (SL) gradually increases for the dual-phase-lag (DPL) model and it is almost constant for the Lord-Shulman (LS) model in the presence of void

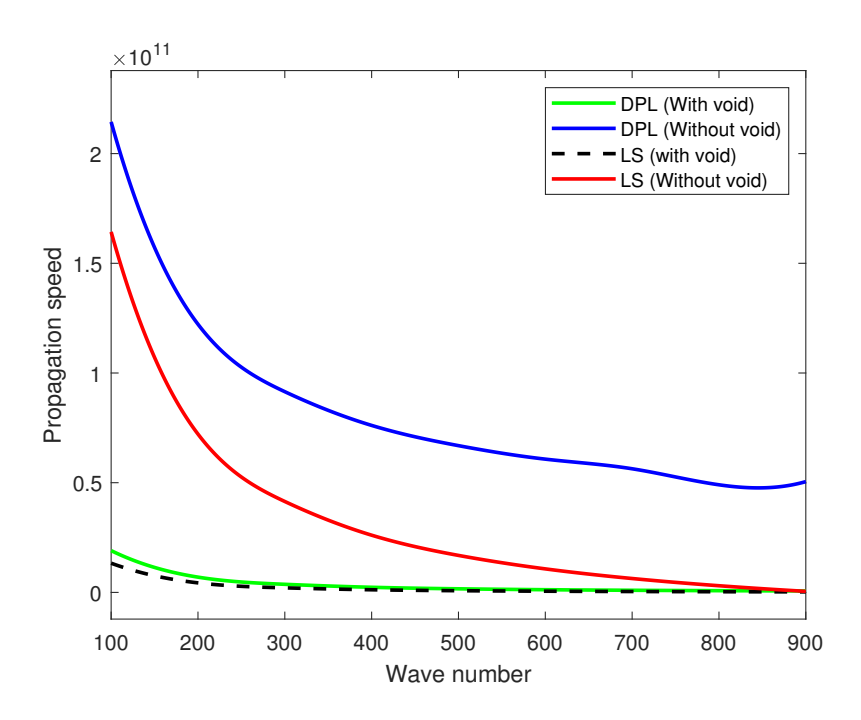


Figure 5: Propagation speed (V) against wave number (k) (for isothermal surface)

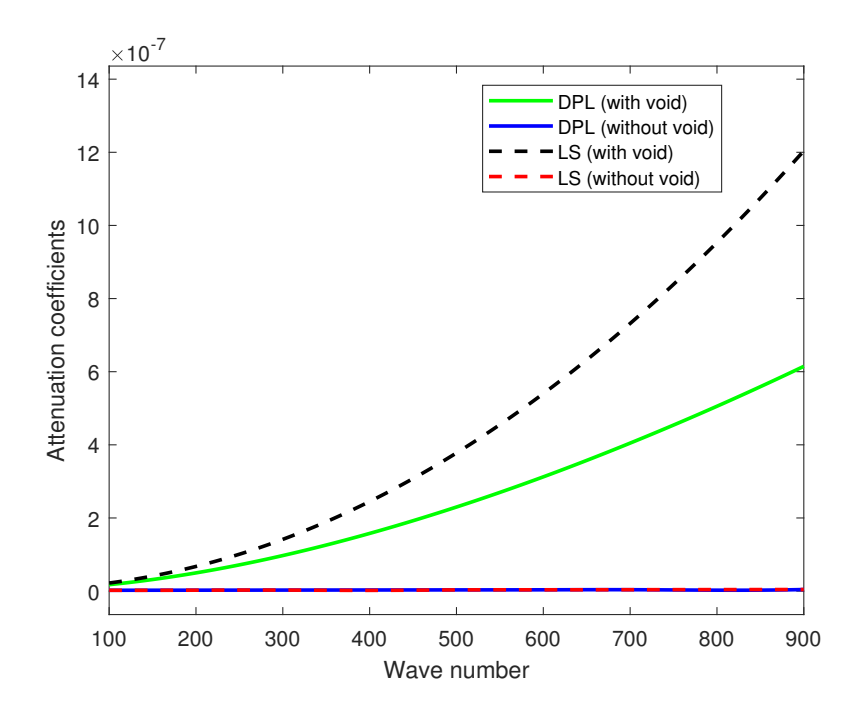


Figure 6: Attenuation coefficient (Q) against wave number (k) (for isothermal surface)

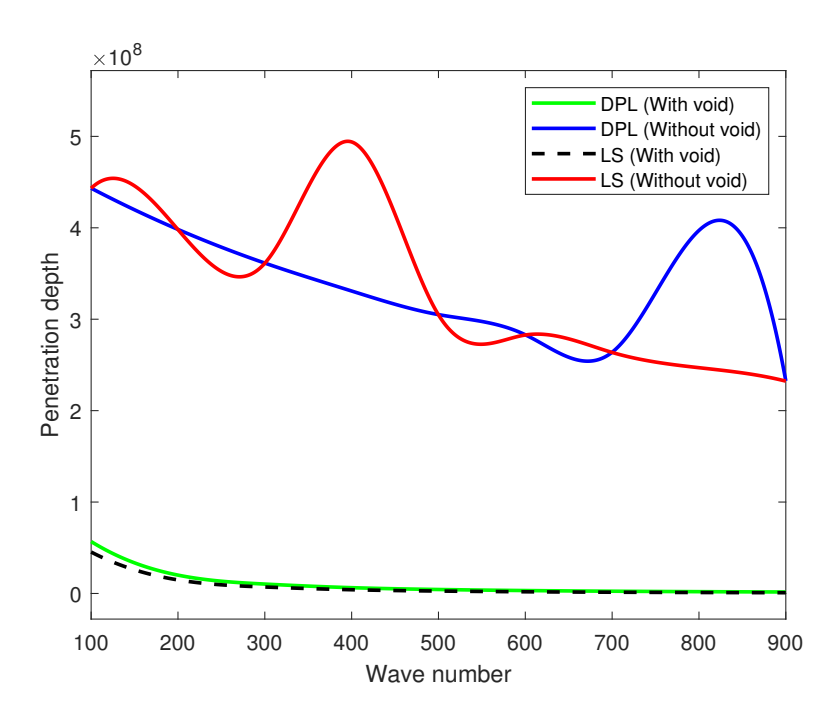


Figure 7: Penetration depth  $(\delta)$  against wave number (k) (for isothermal surface)

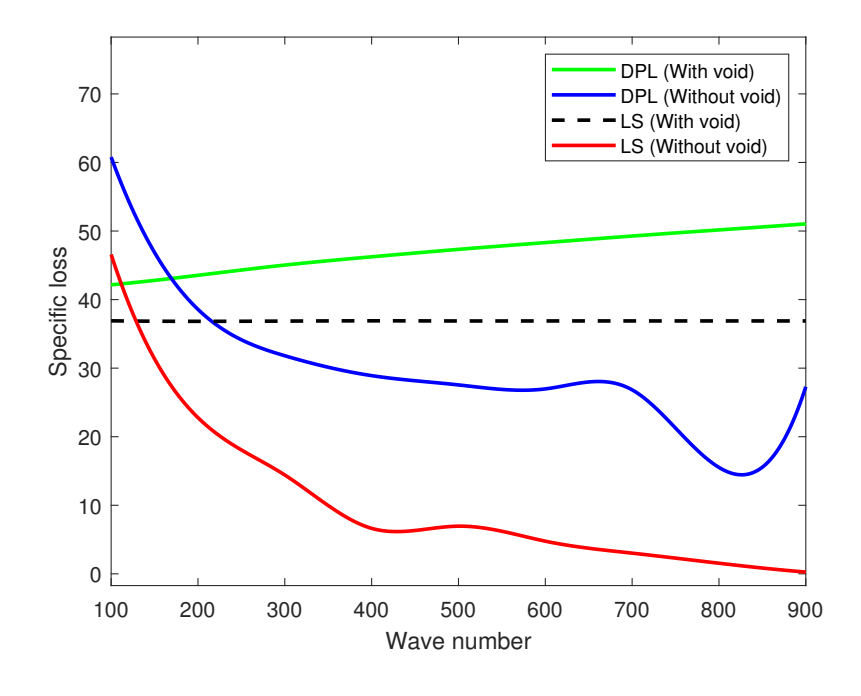


Figure 8: Specific loss (SL) against wave number (k) (for isothermal surface)

parameters.

In figures 9-16, we perform the graphs for propagation speed, attenuation coefficients, penetration depth, and specific loss with respect to wave number (k) for thermoelastic models dual-phase-lag (DPL) model and Lord-Shulman (LS) model for thermally insulated surfaces. Figure 9 illustrates the variation of propagation speed (V) with respect to wave number (k) for thermally insulated surfaces with voids. Initially, it shows a sudden decrease of propagation speed (V) for 100 < k < 300 and a gradual decrease of propagation speed (V) for 300 < k < 900 for both DPL nonlocal and LS nonlocal models. Propagation speed (V) gradually decreases with the increase of wave number (k) for LS local model.

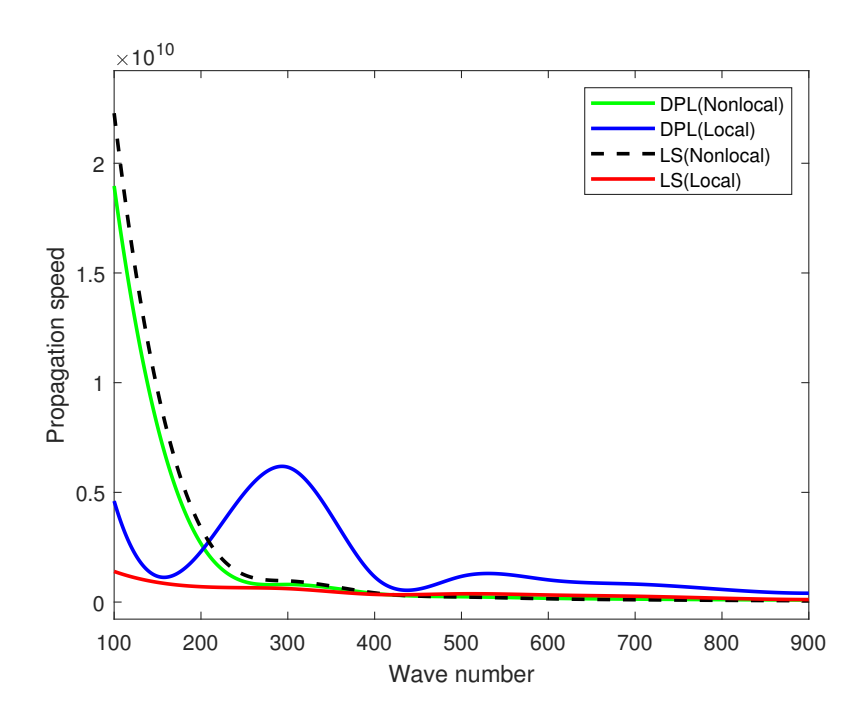


Figure 9: Propagation speed (V) against wave number (k) (for thermally insulated surface)

Figure 10 illustrates the variation of attenuation coefficient (Q) to wave number (k) for thermally insulated surfaces with voids. The attenuation coefficient (Q) for both the DPL nonlocal and LS nonlocal models progressively rises as the wave number (k) grows. Compared to the DPL model, the attenuation coefficient (Q) is higher for the LS model. The attenuation coefficient (Q) increases when nonlocal factors are included.

Figure 11 illustrates the variation of penetration depth  $(\delta)$  with respect to wave number (k) for thermally insulated surfaces with voids. For DPL nonlocal and LS local and nonlocal models, the penetration depth  $(\delta)$  progressively drops as wave number (k) increases. At first, there appears to be a sharp drop in penetration depth  $(\delta)$ . When comparing the DPL model (both local and nonlocal) to the LS model, the penetration depth  $(\delta)$  is larger.

Figure 12 illustrates the variation of specific loss (SL) for wave number (k) for thermally insulated surfaces with voids. For both DPL nonlocal and LS nonlocal models, it first displays a dramatic fall in specific loss (SL) for 100 < k < 300 and a progressive decline in specific loss

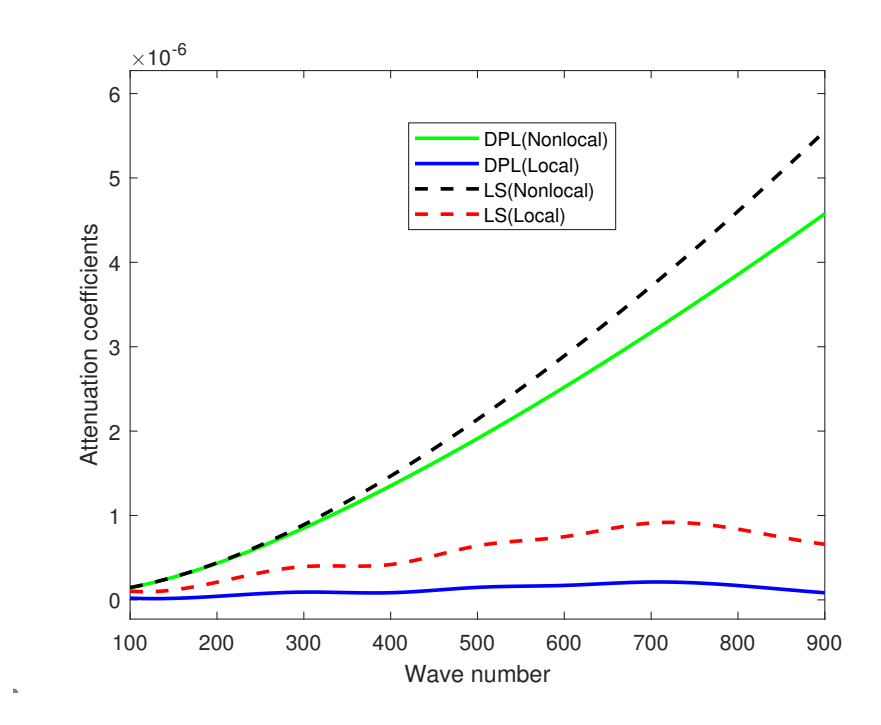


Figure 10: Attenuation coefficient (Q) against wave number (k) (for thermally insulated surface)

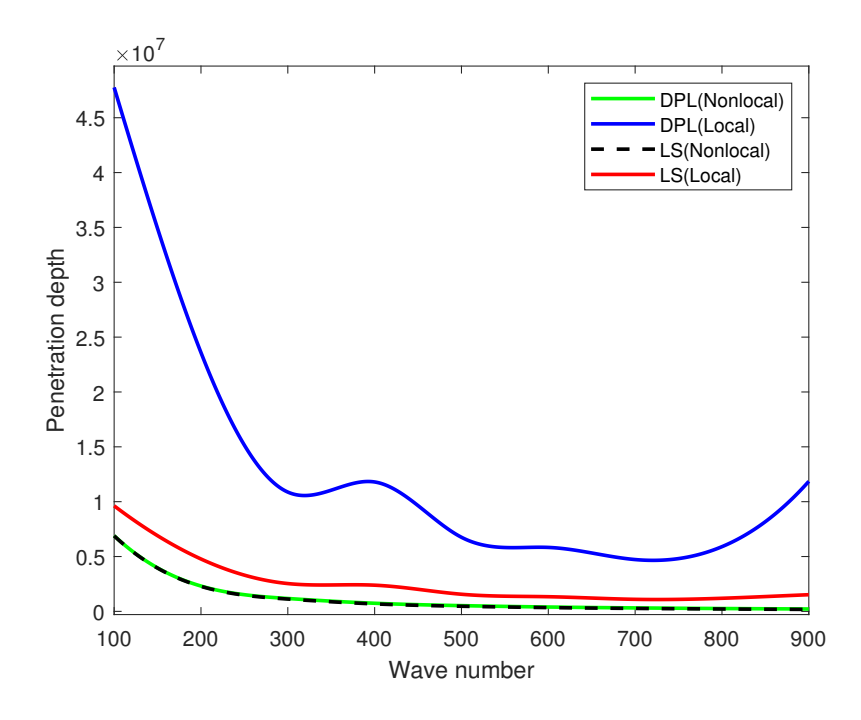


Figure 11: Penetration depth  $(\delta)$  against wave number (k) (for thermally insulated surface)

(SL) for 300 < k < 900. For the range 100 < k < 600, the specific loss (SL) for the LS nonlocal model is higher than that of the DPL nonlocal model. Compared to the DPL nonlocal model, the specific loss (SL) for the range 600 < k < 900 is smaller for the LS nonlocal model. When comparing the LS local model to the DPL local model, the specific loss (SL) is lower.

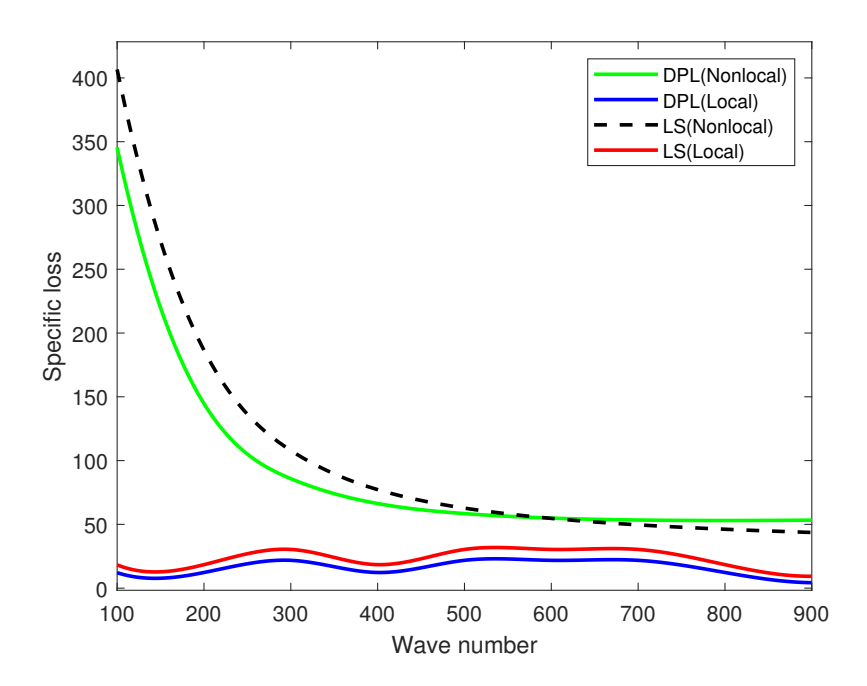


Figure 12: Specific loss (SL) against wave number (k) (for thermally insulated surface)

Figure 13 illustrates the variation of propagation speed (V) for wave number (k) for a thermally insulated surface. Initially, it shows a sudden decrease of propagation speed (V) for 100 < k < 300 and a gradual decrease of propagation speed (V) for 300 < k < 900 for both DPL with void and LS with void models. Propagation speed (V) gradually decreases with the increase of wave number (k) for LS without void model. Propagation speed (V) is greater for LS model in comparison with the DPL model for the absence of void parameters.

Figure 14 illustrates the variation of attenuation coefficient (Q) with respect to wave number (k) for thermally insulated surfaces. The attenuation coefficient (Q) for both the DPL and LS models progressively rises as the wave number (k) grows for the presence of void parameters. Compared to the DPL model, the attenuation coefficient (Q) is higher for the LS model when void parameters are included. The attenuation coefficient (Q) is greater for the DPL model with respect to LS model in the absence of void parameters.

Figure 15 illustrates the variation of penetration depth  $(\delta)$  with respect to wave number (k) for a thermally insulated surface. For DPL with void and LS with void and without void models, the penetration depth  $(\delta)$  progressively drops as wave number (k) increases. At first, there appears to be a sharp drop in penetration depth  $(\delta)$ . When comparing the DPL model (both with void and without void) to the LS model, the penetration depth  $(\delta)$  is larger.

Figure 16 illustrates the variation of specific loss (SL) with respect to wave number (k) for thermally insulated surfaces. For both DPL with void and LS with void models, it first displays

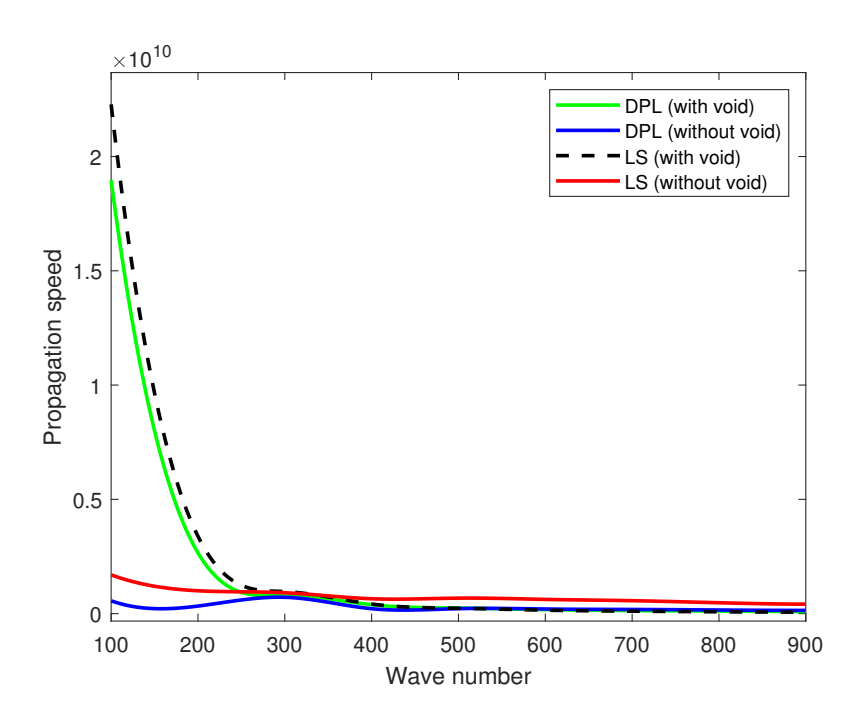


Figure 13: Propagation speed (V) against wave number (k) (for thermally insulated surface)

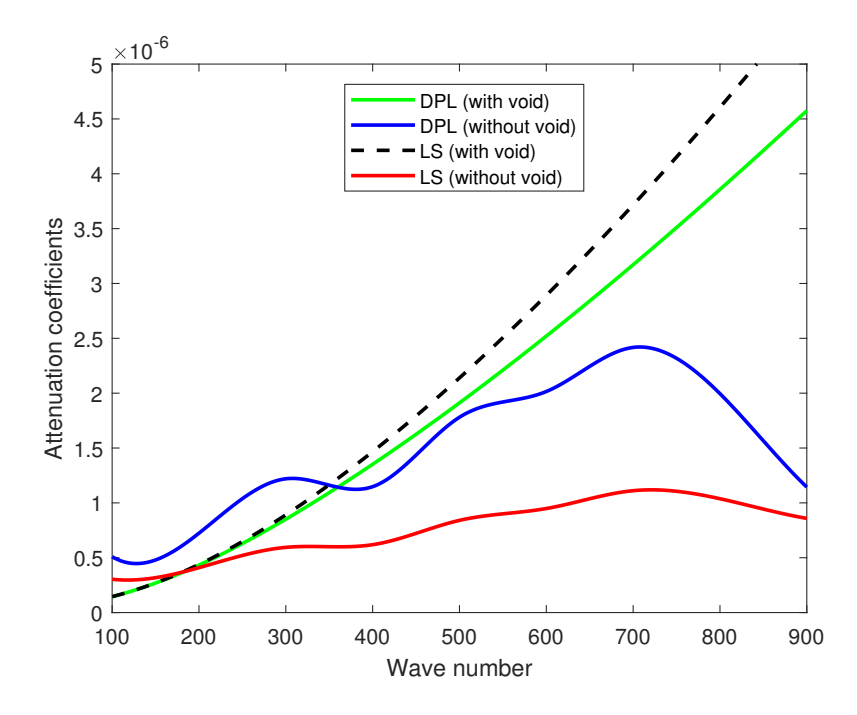


Figure 14: Attenuation coefficient (Q) against wave number (k) (for thermally insulated surface)

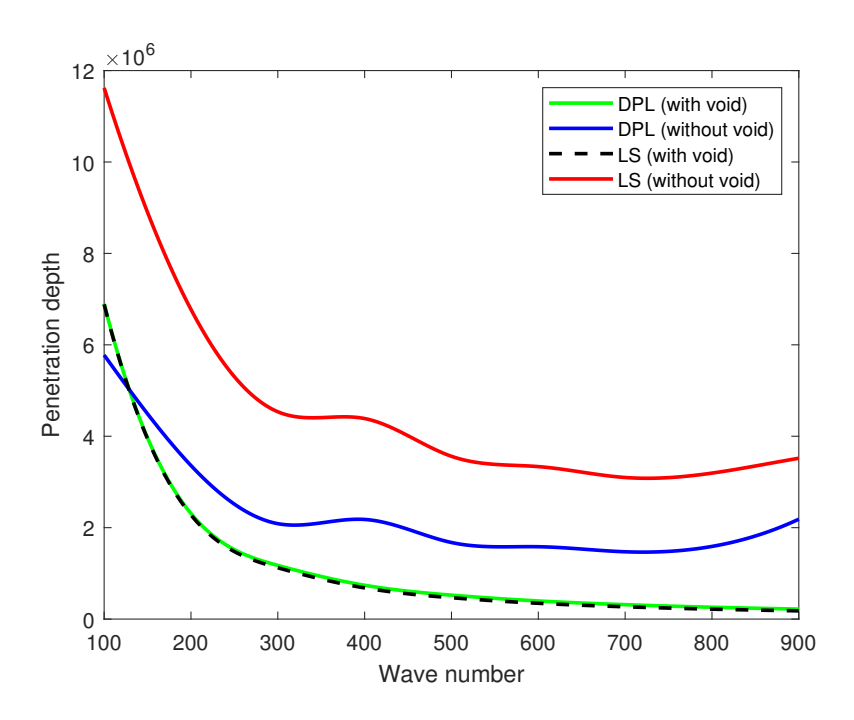


Figure 15: Penetration depth  $(\delta)$  against wave number (k) (for thermally insulated surface)

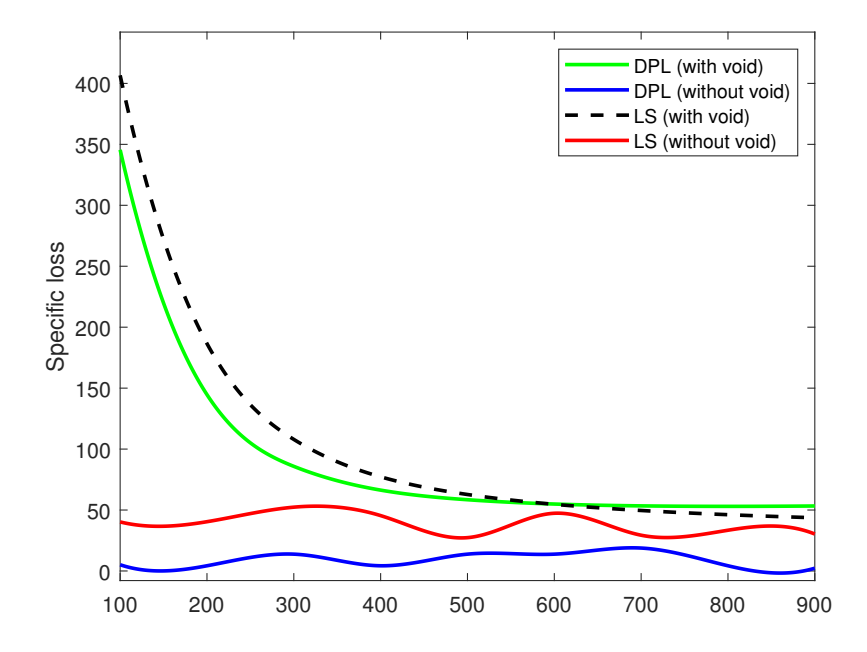


Figure 16: Specific loss (SL) against wave number (k) (for thermally insulated surface)

a dramatic fall in specific loss (SL) for 100 < k < 300 and a progressive decline in specific loss (SL) for 300 < k < 900. For the range 100 < k < 600, the specific loss (SL) for the LS model is higher than that of the DPL model in the presence of void parameters. Compared to the DPL model, the specific loss (SL) for the range 600 < k < 900 is smaller for the LS model in the presence of void parameters. When comparing the LS model to the DPL model, the specific loss (SL) is lower in the absence of void parameters.

Figure 16 illustrates the variation of specific loss (SL) with respect to wave number (k) for thermally insulated surface. For both DPL with void and LS with void models, it first displays a dramatic fall in specific loss (SL) for 100 < k < 300 and a progressive decline in specific loss (SL) for 300 < k < 900. For the range 100 < k < 600, the specific loss (SL) for the LS model is higher than that of the DPL model in the precence of void parameters. Compared to the DPL model, the specific loss (SL) for the range 600 < k < 900 is smaller for the LS model in the precence of void parameters. When comparing the LS model to the DPL model, the specific loss (SL) is lower in the absence of void parameters.

### 12 Conclusions

In this present article, the nonlocal thermoelasticity with double porosity structure has been investigated in the context of the dual-phase-lag (DPL) model and Lord-Shulman (LS) model based on Eringen's nonlocal thermoelasticity theory. To solve this problem, we employ normal mode analysis, and some special cases are discussed.

From the aspect of theoretical, numerical, and graphical observation of the present study, the following conclusions may be inferred:

- (a) Initially, the propagation speed (V) decreases strictly in the absence of nonlocal and void parameters, while it decreases smoothly in the presence of nonlocal and void parameters for isothermal surfaces. For isothermal surfaces, propagation speed becomes stable for higher values of wave number. For thermally insulated surfaces, the DPL and LS models show a dramatic fall in propagation speed (V) for 100 < k < 300 and a progressive decline in propagation speed (V) for 300 < k < 900 due to the impact of nonlocal and void parameters.
- (b) When nonlocal parameters and void parameters are present for an isothermal surface, the attenuation coefficient (Q) increases strictly. The attenuation coefficient is almost constant for DPL and LS models in the absence of nonlocal and void parameters for isothermal surfaces. When nonlocal and void parameters are present for a thermally insulated surface, the DPL model's attenuation coefficient (Q) is smaller than the LS model.
- (c) The penetration depth  $(\delta)$  for an isothermal surface reduces in the presence of nonlocal and void parameters for isothermal surfaces. Penetration depth decreases smoothly for lower values of wave number and then becomes stable for higher values of wave number

in the presence of nonlocal and void parameters for isothermal surfaces. Initially, penetration depth decreases and finally becomes stable due to the important of nonlocal and void parameters for thermally insulated surfaces.

(d) Specific loss increases strictly for the DPL model, while it is almost constant for the LS model in the presence of nonlocal and double void parameters for the isothermal surface. For thermally insulated surfaces, the value of specific loss (SL) in the presence of nonlocal and void parameters is higher than the value of specific loss (SL) in the absence of nonlocal and void parameters. Specific loss shows wave-like bahavior in the absence of nonlocal and void parameters for thermally insulated surfaces.

The concept of porous media is used in many areas of applied science and engineering, namely, filtration, mechanics (acoustics, geomechanics, soil mechanics, rock mechanics), engineering (petroleum engineering, construction engineering), geosciences (hydrogeology, petroleum geology, geophysics), biology and biophysics, and material science. Rayleigh wave propagation has applications in geophysics, earthquake engineering, ultrasonic imaging, etc.

## References

Abouelregal A.E. (2019) "A novel generalized thermoelasticity with higher-order time-derivatives and three-phase lags", *Multidiscipline Modeling in Materials and Structures*, **16**:4, 689-711.https://doi.org/10.1108/MMMS-07-2019-0138.

Biswas S. (2020a) "Surface waves in porous nonlocal thermoelastic orthotropic medium", *Acta Mechanica*, **231**, 2741-2760. https://doi.org/10.1007/s00707-020-02670-2.

Biswas S. (2020b) "Rayleigh waves in a nonlocal thermoelastic layer lying over a nonlocal thermoelastic half-space", *Acta Mechanica*, **231**:10, 4129-4144. https://doi.org/10.1007/s00707-020-02751-2.

Biswas S. (2021) "Thermal shock problem in porous orthotropic medium with three-phase-lag model", *Indian Journal of Physics*, **95**:2. 289-298.https://doi.org/10.1007/s12648-020-01703-9.

Biswas S., Mukhopadhyay B. (2017) "Eigenfunction expansion method to analyze thermal shock behaviour in magneto-thermoelastic orthotropic medium under three theories", *Journal of Thermal Stress*, **41**:3, 366-382. https://doi.org/10.1080/01495739.2017.1393780.

Chandrasekharaiah D.S. (1998) "Hyperbolic thermoelasticity: a review of recent literature", Applied Mechanics Reviews, 51:12, 705-729. https://doi.org/10.1115/1.3098984.

Cowin S.C., Nunziato J.W. (1983) "Linear elastic materials with voids", *Journal of Elasticity*, **13**:2, 125-147. https://doi.org/10.1007/BF00041230.

Chiriță S., Arusoaie A. (2021) "Thermoelastic waves in double porosity materials", European Journal of Mechanics-A/Solids, 86, 104177. https://doi.org/10.1016/j.euromechsol.2020.104177

Eringen A.C., Edelen D.G.B. (1972) "On nonlocal elasticity", *International Journal of Engineering Science*, **10**:3, 233-248. https://doi.org/10.1016/0020-7225(72)90039-0

Eringen A.C. (1974) "Theory of nonlocal thermoelasticity", *International Journal of Engineering Science*, **12**:12, 1063-1077. https://doi.org/10.1016/0020-7225(74)90033-0

Eringen A.C. (1977) "Edge dislocation in nonlocal elasticity", International Journal of Engineering Science, 15:3, 177-183. https://doi.org/10.1016/0020-7225(77)90003-9

Eringen A.C. (1998) "A mixture theory of electromagnetism and superconductivity", *International Journal of Engineering Science*, **36**:5-6, 525-543. https://doi.org/10.1016/S0020-7225(97)00091-8

Green A.E., Lindsay K.A. (1972) "Thermoelasticity", Journal of Elasticity, 2, 1-7. https://doi.org/10.10 Green A.E., Naghdi P.M. (1992) "On undamped heat waves in an elastic solid", Journal of Thermal Stress, 15, 253-264. https://doi.org/10.1080/01495739208946136

Green A.E., Naghdi P.M. (1993) "Thermoelasticity without energy dissipation", *Journal of Elasticity*, **31**, 189-208. https://doi.org/10.1007/BF00044969

Gupta M., Mukhopadhyay S. (2019) "A study on generalized thermoelasticity theory based on nonlocal heat conduction model with dual-phase-lag model", *Journal of Thermal Stress*, **42**:9, 1123-1135. https://doi.org/10.1080/01495739.2019.1614503

Haque I., Biswas S. (2021) "State space approach to characterize Rayleigh waves in a layer lying over a half-space with nonlocal thermoelasticity", *Waves in Random and Complex Media*, **34**:5, 3689-3715. https://doi.org/10.1080/17455030.2021.1983233

Haque I., Biswas S. (2024) "Rayleigh waves in nonlocal porous thermoelastic layer with Green-Lindsay model", Steel and Composite Structures, **50**:2, 123-133. https://doi.org/10.12989/scs.2024.5 Iesan D. (1986) "A theory of thermoelastic materials with voids", Acta Mechanica, **60**:1-2, 67-89. https://doi.org/10.1007/BF01302942

Iesan D., Quintanill R. (2014) "On a Theory of Thermoelastic Materials with a Double Porosity Structure", Journal of Thermal Stresses, 37:9, 1017-1036. https://doi.org/10.1080/01495739.2014 Kalkal K.K., Kadian A., Kumar S. (2021) "Three-phase-lag functionally graded thermoelastic model having double porosity and gravitational effect", Journal of Ocean Engineering and Science, 8:1, 42-54. https://doi.org/10.1016/j.joes.2021.11.005

Khalili N. (2003) "Coupling effects in double porosity media with deformable matrix", Geophysical Research Letters, **30**:22, 2153. https://doi.org/10.1029/2003GL018544

Khalili N., Selvaduri A.P.S. (2003) "A fully coupled constitutive model for thermo-hydromechanical analysis in elastic media with double porosity", *Geophysical Research Letters*, **30**:24, 2268-2271. https://doi.org/10.1029/2003GL018838

Khurana A., Tomar S.K. (2016) "Wave propagation in nonlocal microstretch solid", *Applied Mathematical Modelling*, **40**, 5858-5875. https://doi.org/10.1016/j.apm.2016.01.035

Kolsky H. (1964) "Stress waves in solids", Journal of Sound and Vibration, 1:1, 88-110. https://doi.org/10.1016/0022-460X(64)90008-2

Kumar R., Vohra R., Abo-Dahab S.M. (2018) "Rayleigh waves in thermo elastic medium with double porosity", MOJ Civil Engineering, 4:3, 143-148. https://doi.org/10.15406/mojce.2018.04.0011

Kumar D., Singh D., Tomar S.K., Hirose S., Saitoh T., Furukawa F. (2021) "Waves in nonlocal elastic material with double porosity",  $Archive\ of\ Applied\ Mechanics,\ \mathbf{91},\ 4797-4815.$  https://doi.org/10.1007/s00419-021-02035-8

Lord H.W., Shulman Y. (1967) "A generalized dynamical theory of thermoelasticity", *Journal of the Mechanics and Physics of Solids*, **15**:5, 299-309. https://doi.org/10.1016/0022-5096(67)90024-5

Mahato C.S., Biswas S. (2023) "State space approach to study thermal shock problem in nonlocal thermoelastic medium with double porosity", *Journal of Thermal Stresses*, **46**:5, 415-443. https://doi.org/10.1080/01495739.2023.2173689

Mahato C.S., Biswas S. (2024a) "Thermomechanical interactions in nonlocal thermoelastic medium with double porosity structure", *Mechanics of Time-Dependent Materials*, **28**, 1073-1110. https://doi.org/10.1007/s11043-024-09669-5

Mahato C.S., Biswas S. (2024b) "State Space Approach to Characterize Rayleigh Waves in Nonlocal Thermoelastic Medium with Double Porosity under Three-Phase-Lag Model", Computational Mathematics and Mathematical Physics, 64:3, 555-584. https://doi.org/0.1134/S096554252403006

Mittal G., Kulkarni V. (2018) "Dual-phase-lag thermoelastic problem in finite cylindrical domain with relaxation time", *Multidiscipline Modeling in Materials and Structures*, **14**:5, 837-856. https://doi.org/10.1108/MMMS-03-2018-0041

Mondal S., Sarkar N., Sarkar N. (2019) "Waves in dual-phase-lag thermoelastic materials with voids based on Eringen's nonlocal elasticity", *Journal of Thermal Stress*, **42**:8, 1035-1050. https://doi.org/10.1080/01495739.2019.1591249

Nunziato J.W., Cowin S.C. (1979) "A Nonlinear Theory of Elastic Materials with Voids", Arch. Rat. Mech. Anal., 72:2, 175-201. https://doi.org/10.1007/BF00249363.

Ostoja-Starzewski M. (2009) "Continuum mechanics models of fractal porous media: Integral relations and extremum principles", *Journal of Mechanics of Materials and Structures*, 4:5, 901-912. https://doi.org/10.2140/jomms.2009.4.901.

Pramanik A.S., Biswas S. (2020) "Surface waves in nonlocal thermoelastic medium with state approach", *Journal of Thermal Stress*, **43**:6, 667-686. https://doi.org/10.1080/01495739.2020.1734129

Puri P., Cowin S.C. (1985) "Plane waves in linear elastic materials with voids", *Journal of Elasticity*, **15**:2, 167-183. https://doi.org/10.1007/BF00041991

Roy Choudhuri S.K. (2007) "On a thermoelastic three-phase-lag model", *Journal of Thermal Stresses*, **30**:3, 231-238. https://doi.org/10.1080/01495730601130919

Sarkar N., Tomar S.K. (2019) "Plane waves in nonlocal thermoelastic solid with voids", Journal of Thermal Stress, 42:5, 580-606. https://doi.org/10.1080/01495739.2018.1554395

Sherief H., Saleh H. (2005) "A half-space problem in the theory of generalized thermoelastic

diffusion", International Journal of Solids and Structures, **42**:15, 4484-4493. https://doi.org/10.1016/j.ijsol Singh D., Kumar D., Tomar S.K. (2020) "Plane harmonic waves in thermoelastic solid with

double porosity", Mathematics and Mechanics of Solids, 25:4, 869-886. https://doi.org/10.1177/108128651

Tzou D.Y. (1995) "A unique field approach for heat conduction from macro to micro scales", *Journal of Heat Transfer*, **117**:1, 8-16. https://doi.org/10.1115/1.2822329.

Zhou Z.G., Liang J., Wu L.Z. (2006) "The nonlocal theory solution of a mode-I crack in functionally graded materials subjected to harmonic stress waves", *Journal of Mechanics of Materials and Structures*, **1**:3, 447-470. https://doi.org/10.2140/jomms.2006.1.447.

## Appendix

```
N_1 = \frac{p_{30} + p_{56}}{r}
 N_2 = \frac{p_{31} + p_{57} + p_{71} + s_{10} + s_{24}}{p_{31} + p_{57} + p_{71} + s_{10} + s_{24}}
N_3 = \frac{p_{32} + p_{58} + p_{72} + s_{11} + s_{25}}{2}
N_4 = \frac{p_{33} + p_{59} + p_{73} + s_{12} + s_{26}}{p_{17}}
N_5 = \frac{p_{34} + p_{74} + s_{13} + s_{27}}{n_{17}},
p_1 = a_1 + a_6, p_2 = a_1 a_6, p_3 = a_{21} + a_{25}, p_4 = a_{21} a_{25} - a_{22} a_{27}, p_5 = a_{17} a_{25} + a_{18}, p_6 = a_{18} a_{25} - a_{22} a_{26},
p_7 = a_{17}a_{27} - a_{26}, \ p_8 = a_{18}a_{27} - a_{26}a_{21}, \ p_9 = a_{20}a_{25} - a_{22}a_{23}, \ p_{10} = a_{20}a_{27} - a_{21}a_{23}, \ p_{11} = a_{23}a_{17},
p_{12} = a_{20}a_{26} - a_{23}a_{18}, p_{13} = a_{1}a_{8}, p_{14} = a_{1}a_{9}, p_{15} = a_{1}a_{10}, p_{16} = -a_{23}a_{17}, p_{17} = 1 - a_{13}a_{17},
p_{18} = p_3 + a_{11} - p_5 a_{13} - a_{14} a_{17}, p_{19} = p_4 + p_3 a_{11} - p_6 a_{13} - p_5 a_{14} + p_7 a_{16}, p_{20} = a_{11} p_4 - a_{14} p_6 + a_{16} p_8,
p_{21} = a_{12} - a_{20}p_{13}, p_{22} = a_{12}p_3 - p_9p_{13} - a_{14}a_{20} - a_{16}a_{23}, p_{23} = a_{12}p_4 - a_{14}p_9 + a_{16}p_{10},
p_{24} = a_{12}a_{17} - a_{20}, p_{25} = a_{12}p_5 - a_{11}a_{20} + a_{16}p_{16} - p_9, p_{26} = a_{12}p_6 - a_{11}p_9 + a_{16}p_{12}, p_{27} = a_{23} + a_{13}p_{16},
p_{28} = a_{12}p_7 - p_{10} + a_{11}a_{23} + a_{13}p_{12} + a_{14}p_{16}, \ p_{29} = a_{12}p_8 - a_{11}p_{10} + a_{14}p_{12}, \ p_{30} = p_{18} + p_1p_{17} - a_{14}p_{16}
a_8p_{21} + a_9p_{24} - a_{10}p_{27}, p_{31} = p_2p_{17} + p_{19} + p_1p_{18} - a_8p_{22} - p_{13}p_{21} + a_9p_{25} + p_{14}p_{24} - a_{10}p_{28} - p_{15}p_{27},
p_{32} = p_{20} + p_1 p_{19} + p_2 p_{18} - a_8 p_{23} - p_{13} p_{22} + a_9 p_{26} + p_{14} p_{25} - a_{10} p_{29} - p_{15} p_{28}, \ p_{33} = p_1 p_{20} + p_{10} p_{20} +
p_2p_{19} - p_{13}p_{23} + p_{14}p_{26} - p_{15}p_{29}, p_{34} = p_2p_{20}, p_{35} = a_{19}a_{25} - a_{22}a_{24}, p_{36} = a_{19}a_{27} - a_{21}a_{24},
p_{37} = a_{19}a_{26} - a_{18}a_{24}, \ p_{38} = -a_{2}a_{7}, \ p_{39} = a_{2}a_{8}, \ p_{40} = -a_{2}a_{9}, \ p_{41} = a_{2}a_{10}, \ p_{42} = -a_{17}a_{24},
p_{43} = a_{17}a_{24}, p_{44} = 1 - a_{13}a_{17}, p_{45} = a_{11} + p_3 - a_{13}p_5 - a_{14}a_{17}, p_{46} = a_{11}p_3 - a_{13}p_6 - a_{14}p_5 + a_{16}p_7,
p_{47} = a_{11}p_4 - a_{14}p_6 + a_{16}p_8, \, p_{48} = a_{15} - a_{13}a_{19}, \, p_{49} = a_{15}p_3 - a_{13}p_{35} - a_{14}a_{19} - a_{16}a_{24}, \, p_{50} = a_{15}p_4 - a_{16}a_{24}, \, p_{50} = a
a_{14}p_{35} + a_{16}p_{36}, p_{51} = a_{15}a_{17} - a_{19}, p_{52} = a_{15}p_5 - p_{35} - a_{11}a_{19} + a_{16}p_{42}, p_{53} = a_{15}p_6 - a_{11}p_{35} + a_{16}p_{37},
p_{54} = a_{15}p_7 - p_{36} + a_{11}a_{24} + a_{13}p_{37} - a_{14}p_{43}, \ p_{55} = a_{15}p_8 - a_{11}p_{36} + a_{14}p_{37}, \ p_{56} = p_{38}p_{44},
p_{57} = p_{38}p_{45} + p_{39}p_{48} + p_{40}p_{51} - a_{13}p_{41}p_{43} + a_{24}p_{41}, p_{58} = p_{38}p_{46} + p_{39}p_{49} + p_{40}p_{52} + p_{41}p_{54},
p_{59} = p_{38}p_{47} + p_{39}p_{50} + p_{40}p_{53} + p_{41}p_{55}, p_{60} = a_{19}a_{23} - a_{20}a_{24}, p_{61} = a_{12} - a_{13}a_{20}, p_{62} = a_{12}a_{13}a_{12}
a_{12}p_3 - a_{13}p_9 - a_{14}a_{20} - a_{16}a_{23}, \ p_{63} = a_{12}p_4 - a_{14}p_9 + a_{16}p_9, \ p_{64} = a_{15} - a_{13}a_{19}, \ p_{65} = a_{15}p_3 - a_{13}p_{35} - a_{15}p_3 - a
a_{14}a_{19} - a_{16}a_{24}, p_{66} = a_{15}p_4 - a_{14}p_{35} + a_{16}p_{36}, p_{67} = a_{15}a_{20} - a_{12}a_{19}, p_{68} = a_{15}p_9 - a_{12}p_{35} + a_{16}p_{60},
p_{69} = a_{12}a_{24} + a_{13}p_{60} - a_{15}a_{23}, p_{70} = a_{15}p_{10} - a_{12}p_{36} + a_{14}p_{60}, p_{71} = a_3a_7p_{61} - a_3p_{64}, p_{72} = a_{15}p_{10} - a_{1
a_3a_7p_{62} - a_3p_{65} - a_3a_6p_{64} + a_3a_9p_{67} - a_3a_{10}p_{69}, p_{73} = a_3a_7p_{63} - a_3p_{66} - a_3a_6p_{65} + a_3a_9p_{68} - a_3a_{10}p_{70},
p_{74} = -a_3 a_6 p_{66}, s_1 = a_{12} a_{17} - a_{20}, s_2 = a_{12} p_5 - p_9 - a_{16} p_{11} - a_{11} a_{20}, s_3 = a_{12} p_6 - a_{11} p_9 + a_{16} p_{12}, s_4 = a_{12} a_{12} a_{13} - a_{12} a_{14} a_{15} + a_{15} a_{15}
a_{15}a_{17} - a_{19}, s_5 = a_{15}p_5 - p_{35} - a_{11}a_{19} - a_{16}p_{43}, s_6 = a_{15}p_6 - a_{11}p_{35} + a_{16}p_{37}, s_7 = a_{15}a_{20} - a_{12}a_{19},
s_8 = a_{12}a_{17}a_{24} - a_{15}a_{23} + p_{60}, \ s_9 = a_{15}p_{12} - a_{12}p_{37} + a_{11}p_{60}, \ s_{10} = a_4s_4 - a_4a_7s_1, \ s_{11} = a_4s_5 + a_{11}a_{12}a_{13} + a_{12}a_{13}a_{14} + a_{12}a_{15}a_{15}a_{15} + a_{12}a_{15}a_{15}a_{15}a_{15}a_{15}a_{15}a_{15}a_{15}a_{15}a_{15}a_{15}a_{15}a_{15}a_{15}a_{15}a_{15}a_{15}a_{15}a_{15}a_{15}a_{15}a_{15}a_{15}a_{15}a_{15}a_{15}a_{15}a_{15}a_{15}a_{15}a_{15}a_{15}a_{15}a_{15}a_{15}a_{15}a_{15}a_{15}a_{15}a_{15}a_{15}a_{15}a_{15}a_{15}a_{15}a_{15}a_{15}a_{15}a_{15}a_{15}a_{15}a_{15}a_{15}a_{15}a_{15}a_{15}a_{15}a_{15}a_{15}a_{15}a_{15}a_{15}a_{15}a_{15}a_{15}a_{15}a_{15}a_{15}a_{15}a_{15}a_{15}a_{15}a_{15}a_{15}a_{15}a_{15}a_{15}a_{15}a_{15}a_{15}a_{15}a_{15}a_{15}a_{15}a_{15}a_{15}a_{15}a_{15}a_{15}a_{15}a_{15}a_{15}a_{15}a_{15}a_{15}a_{15}a_{15}a_{15}a_{15}a_{15}a_{15}a_{15}a_{15}a_{15}a_{15}a_{15}a_{15}a_{15}a_{15}a_{15}a_{15}a_{15}a_{15}a_{15}a_{15}a_{15}a_{15}a_{15}a_{15}a_{15}a_{15}a_{15}a_{15}a_{15}a_{15}a_{15}a_{15}a_{15}a_{15}a_{15}a_{15}a_{15}a_{15}a_{15}a_{15}a_{15}a_{15}a_{15}a_{15}a_{15}a_{15}a_{15}a_{15}a_{15}a_{15}a_{15}a_{15}a_{15}a_{15}a_{15}a_{15}a_{15}a_{15}a_{15}a_{15}a_{15}a_{15}a_{15}a_{15}a_{15}a_{15}a_{15}a_{15}a_{15}a_{15}a_{15}a_{15}a_{15}a_{15}a_{15}a_{15}a_{15}a_{15}a_{15}a_{15}a_{15}a_{15}a_{15}a_{15}a_{15}a_{15}a_{15}a_{15}a_{15}a_{15}a_{15}a_{15}a_{15}a_{15}a_{15}a_{15}a_{15}a_{15}a_{15}a_{15}a_{15}a_{15}a_{15}a_{15}a_{15}a_{15}a_{15}a_{15}a_{15}a_{15}a_{15}a_{15}a_{15}a_{15}a_{15}a_{15}a_{15}a_{15}a_{15}a_{15}a_{15}a_{15}a_{15}a_{15}a_{15}a_{15}a_{15}a_{15}a_{15}a_{15}a_{15}a_{15}a_{15}a_{15}a_{15}a_{15}a_{15}a_{15}a_{15}a_{15}a_{15}a_{15}a_{15}a_{15}a_{15}a_{15}a_{15}a_{15}a_{15}a_{15}a_{15}a_{15}a_{15}a_{15}a_{15}a_{15}a_{15}a_{15}a_{15}a_{15}a_{15}a_{15}a_{15}a_{15}a_{15}a_{15}a_{15}a_{15}a_{15}a_{15}a_{15}a_{15}a_{15}a_{15}a_{15}a_{15}a_{15}a_{15}a_{15}a_{15}a_{15}a_{15}a_{15}a_{15}a_{15}a_{15}a_{15}a_{15}a_{15}a_{15}a_{15}a_{15}a_{15}a_{15}a_{15}a_{15}a_{15}a_{15}a_{15}a_{15}a_{15}a_{15}a_{15}a_{15}a_{15}a_{15}a_{15}a_{1
a_4a_6s_4 - a_4a_7s_2 - a_4a_8s_7 + a_4a_{10}s_8, \, s_{12} = a_4s_6 + a_4a_6s_5 - a_4a_7s_3 - a_4a_8p_{68} + a_4a_{10}s_{10}, \, s_{13} = a_4a_6s_6,
s_{14} = -a_{23} - a_{13}p_{11}, \ s_{15} = a_{12}p_7 + p_{10} - a_{11}a_{23} + a_{13}p_{12} - a_{14}p_{11}, \ s_{16} = a_{12}p_8 + a_{11}p_{10} + a_{14}p_{12},
s_{17} = a_{13}p_{42} + a_{24}, \ s_{18} = a_{15}p_7 - p_{36} + a_{11}a_{24} + a_{13}p_{37} + a_{14}p_{42}, \ s_{19} = a_{15}p_8 - a_{11}p_{36} + a_{14}p_{37},
s_{20} = a_{12}a_{24} - a_{15}a_{23} + a_{13}p_{60}, \ s_{21} = a_{15}p_{10} - a_{12}p_{36} + a_{14}p_{60}, \ s_{22} = p_{60} - a_{15}p_{11} - a_{12}p_{42},
s_{23} = a_{15}p_{12} - a_{12}p_{37} + a_{11}p_{60}, s_{24} = a_5a_7s_{14} - a_5s_{17}, s_{25} = a_5a_7s_{15} - a_5s_{18} - a_6s_{17} + a_5a_8s_{20} - a_5a_9s_{22},
s_{26} = a_5 a_7 s_{16} - a_5 s_{19} - a_5 a_6 s_{18} + a_5 a_8 s_{21} - a_5 a_9 s_{23}, \ s_{27} = -a_5 a_6 s_{19}.
```

$$a_0 = \mu - \rho \varepsilon^2 k^2 c^2, \ a_1 = \frac{\rho k^2 c^2 (1 + \varepsilon^2 k^2) - k^2 (\lambda + 2\mu)}{a_0}, \ a_2 = \frac{ik(\lambda + \mu)}{a_0}, a_3 = \frac{ikh}{a_0}, \ a_4 = \frac{ikd}{a_0}, \ a_5 = \frac{-ik\beta}{a_0}, \ b_0 = \lambda + 2\mu - \rho \varepsilon^2 k^2 c^2, \ a_6 = \frac{\rho k^2 c^2 (1 + \varepsilon^2 k^2) - \mu k^2}{b_0}, \ a_7 = \frac{ik(\lambda + \mu)}{b_0}, \ a_8 = \frac{h}{b_0}, \ a_9 = \frac{d}{b_0}, \ a_{10} = \frac{-\beta}{b_0}, \ c_0 = \alpha - \chi_1 \varepsilon^2 k^2 c^2, \ a_{11} = \frac{\chi_1 k^2 c^2 (1 + \varepsilon^2 k^2) - \alpha k^2 - m}{c_0}, \ a_{12} = \frac{-h}{c_0}, \ a_{13} = \frac{b_1}{c_0}, \ a_{14} = \frac{-(b_1 k^2 + l)}{c_0}, \ a_{15} = \frac{-ikh}{c_0}, \ a_{16} = \frac{\gamma_1}{c_0}, \ a_{16} = \frac{\gamma_1}{c_0},$$

$$\begin{array}{l} d_0 = \gamma - \chi_2 \varepsilon^2 k^2 c^2, \; a_{17} = \frac{b_1}{d_0}, \; a_{18} = \frac{-(b_1 k^2 + l)}{d_0}, \; a_{19} = \frac{-ikd}{d_0}, \; a_{20} = \frac{-d}{d_0}, \; a_{21} = \frac{\chi_2 k^2 c^2 (1 + \varepsilon^2 k^2) - \alpha k^2 - m}{c_0}, \\ a_{22} = \frac{\gamma_2}{d_0}, \; \tau_1 = 1 - ikc\tau_q, \; \tau_2 = 1 - ikc\tau_T, \; e_0' = K\tau_2, \; a_{23} = \frac{ikcT_0 \beta \tau_1}{e_0'}, \; a_{24} = \frac{-k^2 cT_0 \beta \tau_1}{e_0'}, \; a_{25} = \frac{ikc\rho C_v \tau_1}{e_0'} - k^2, \; a_{26} = \frac{ikcT_0 \gamma_1 \tau_1}{e_0'}, \; a_{27} = \frac{ikcT_0 \gamma_2 \tau_1}{e_0'}. \\ F_n = \lambda_n [a_{10}(\lambda_n^2 + a_1) - a_5 a_7], \; G_n = (a_5 - a_2 a_{10})\lambda_n^2 + a_5 a_6, \; J_n = a_{16}(\lambda_n^2 + a_1) - a_5 a_{15}, \\ K_n = (a_5 a_{12} - a_2 a_{16})\lambda_n, \; L_n = a_3 a_{16} - a_5(\lambda_n^2 + a_{11}), \; P_n = a_4 a_{16} - a_5(a_{13}\lambda_n^2 + a_{14}), \; Q_n = a_{22}(\lambda_n^2 + a_1) - a_5 a_{19}, \; R_n = (a_5 a_{20} - a_2 a_{22})\lambda_n, \; T_n = a_3 a_{22} - a_5(a_{17}\lambda_n^2 + a_{18}), \; U_n = a_4 a_{22} - a_5(\lambda_n^2 + a_{21}), \\ x_n = \frac{-F_n}{G_n}, \; y_n = \frac{x_n(P_n R_n - k_n U_n) + (P_n Q_n - J_n U_n)}{L_n U_n - P_n T_n}, \; z_n = \frac{-(J_n + x_n k_n + y_n L_n)}{P_n}, \; f_n = ik\lambda - \lambda_n x_n(\lambda + 2\mu) + hy_n + dz_n - \beta e_n, \; g_n = \mu(ikx_n - \lambda_n), \; l_n = \lambda_n(\alpha y_n + b_1 z_n), \; m_n = \lambda_n(b_1 y_n + \gamma z_n), \; r_n = \lambda_n e_n, \\ e_n = \frac{a_{23} x_n \lambda_n - a_{24} - a_{26} y_n - a_{27} z_n}{\lambda_n^2 + a_{25}}; (n = 1, 2, 3, 4, 5). \end{array}$$